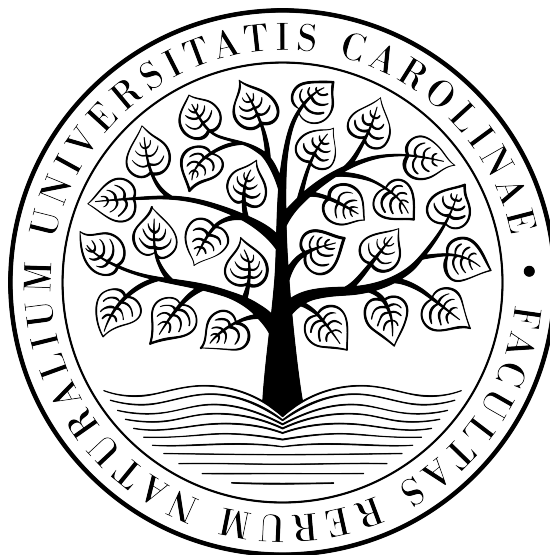


Charles University
Faculty of Science



Bc. Lenka Šimonová

Interaction of a surface marker of immune cells with low-molecular weight ligands and their polymer conjugates

Interakce povrchového markeru imunitních buněk
s nízkomolekulárními ligandy a jejich
polymerními konjugáty

Diploma thesis

Supervisor: doc. RNDr. Jan Konvalinka, CSc.

Consultant: Mgr. Kristýna Blažková

Study program: Chemistry

Study branch: Biophysical chemistry

Prague 2019

The experimental part of this work was done at Institute of Organic Chemistry and Biochemistry (IOCB) AS CR, v.v.i. in the laboratory of Dr. Jan Konvalinka.

Prohlašuji, že jsem závěrečnou práci zpracovala samostatně a že jsem uvedla všechny použité informační zdroje a literaturu. Tato práce ani její podstatná část nebyla předložena k získání jiného nebo stejného akademického titulu.

Praha, 3. 5. 2019

Lenka Šimonová

Acknowledgement

In the first place, I would like to thank Jan Konvalinka for accepting me into his laboratory full of great people. I would like to thank Jan Konvalinka and Pavel Šácha for their advice, and for always being ready to give me a new (lab) challenge during my studies.

Great thanks belong to Kristýna Blažková, who taught me new techniques, patiently explained new concepts, managed to cooperate with me and in the end carefully reviewed this thesis.

I would like to thank all the colleagues in our lab, namely Jana Beranová for our talks and great support, Káťa Rojíková for all the help with DIANA experiments, Martin Pehr, just for being another oompa-loompa (chocolate?), Jana Bimča Starková for tissue culture tips & tricks and together with Karolína Šrámková for the lab maintenance and helping hands, Michal Svoboda for his silly jokes and story about ants.

Special thanks belong to my boyfriend Honza, who was patiently listening, whenever I felt depressive during writing my thesis. And for solving my T_EXnical issues. And for all those cups of tea and coffee.

I would like to also thank my family – my loving parents and brothers, and my friends for their support.

Many thanks belong also to my deciphering and exit-game team *Život je změna spinu*. I would not have managed to write this thesis without the experiences of total despair of the piece of paper full of weird pictures/signs/letters, frosty night and sleepiness.

*Become the legend,
now starts the age undreamed of,
let's go to the dark,
let me tell you of the night of high adventure.
TMOU! anthem*

Abstract

Millions of people worldwide die of cancer every year. In the last decade, immunotherapy offered new treatment options achieving long-lasting remissions in a number of patients. Several new immunotherapy-based drugs have been approved by Food and Drug Administration. However, majority of patients either do not respond or soon relapse. Combination of therapies as well as exploring new immune checkpoints seems promising.

This thesis focuses on the new immunotherapeutic target CD73. CD73 is membrane ectonucleotidase, widely expressed on the regulatory leukocytes and on cancer cells. The enzymatically active CD73 contributes to the tumour microenvironment by production of immunosuppressive adenosine. This novel immune checkpoint is being intensively studied. This thesis aims on development of new approaches for targeting and inhibition of CD73.

Soluble recombinant CD73 (rhCD73) was prepared in mammalian expression system and transfectants stably expressing membrane-bound CD73 were prepared as well. Inhibitors necessary for both of my goals have been designed based on published inhibitor of CD73.

Development and evaluation of novel antibody mimetic for CD73 characterisation was done. The so-called iBody, HPMA polymer conjugate decorated with CD73 inhibitor for targeting, fluorophore for visualisation and biotin for immobilisation of the polymer conjugate, was developed and validated in different biochemical methods as well as in cell assays.

Furthermore, the development of high-throughput assay (HTS) is described for CD73 inhibitor screening based on DIANA method (DNA-linked Inhibitor Antibody Assay). The conditions of the method were optimised and first inhibitor testing has been performed.

The findings in this thesis allow us to further develop nanochemical tools that are able to target and modulate immunosuppressive components of tumour microenvironment.

Key words: receptor, ligand, recombinant protein, polymer conjugate, HPMA, fluorescence, immunotherapy, CD73, DIANA

Abstrakt

Každý rok zemřou na rakovinu miliony lidí po celém světě. V posledním desetiletí nabízí imunoterapie nové léčebné přístupy s dlouhotrvajícími remisemi u řady pacientů. Úřad pro kontrolu potravin a léčiv (Food and Drug Administration, FDA) schválil několik nových léčiv založených na imunoterapii. Nicméně, pro většinu pacientů je tato léčba neúčinná, případně se nemoc brzy znovu projeví. Slibně se dnes jeví hledání a zkoumání nových kontrolních bodů imunitního systému a léčba kombinující cílení různých těchto bodů.

Tato práce se zaměřuje na nový cíl imunoterapie – CD73. CD73 je membránová ektonukleotidasa, vysoce exprimovaná v regulačních leukocytech a v rakoviných buňkách. Svojí enzymatickou aktivitou, tvorbou imunosupresivního adenosinu, přispívá k vytváření nádorového mikroprostředí. Tento nový kontrolní bod imunitního systému je proto intenzivně studován. Cílem této práce je vývoj nových metod cílení a inhibice CD73.

Rozpustná forma rekombinantní lidské CD73 (rhCD73) byla připravena v savčím expresním systému, dále byla také připravena buněčná linie stabilně exprimující CD73 na svém povrchu. Inhibitory potřebné pro oba zmíněné cíle byly navrženy na základě struktury publikovaného inhibitoru CD73.

Protilátkové mimetikum pro charakterisaci CD73 bylo vyvinuto a evaluováno. Tento HPMa polymerní konjugát, tak zvané *iBody*, dekorovaný inhibitorem pro cílení CD73, fluoroforem pro visualisaci a biotinem pro imobilizaci, byl charakterisován různými biochemickými metodami a testovaný v buněčných experimentech.

Dále byla vyvinuta metoda pro vysokokapacitní testování inhibitorů CD73 založená na metodě DIANA (DNA-linked Inhibitor Antibody Assay). Podmínky metody byly optimalisovány a proběhlo první vysokokapacitní testování inhibitorů knihovny malých molekul.

Výsledky této práce umožňují další vývoj nanochemických nástrojů schopných cílit a modulovat imunosupresivní mikroprostředí nádoru.

Klíčová slova: receptor, ligand, rekombinantní protein, polymerní konjugát, HPMa, fluorescence, imunoterapie, CD73, DIANA

Contents

Abstract	4
List of Abbreviations	9
Introduction	11
1 Cancer treatment overview	12
1.1 Classic approaches to cancer treatment	12
1.2 Immune system	12
1.3 Immunotherapy	12
1.3.1 Vaccination	13
1.3.2 Adoptive T cell therapy	14
1.3.3 Bispecific T cell engager	14
1.3.4 Oncolytic viruses	14
1.3.5 Checkpoint inhibitors	15
2 Tumour microenvironment	15
2.1 Cancer associated fibroblasts	16
2.2 Immune cells in tumour microenvironment	16
2.3 Purinergic signalling	17
2.3.1 Mechanism of ATP release	17
2.3.2 Enzymes involved in purinergic signalling	17
2.3.3 Purine receptors	17
3 Ecto-5'-nucleotidase	18
3.1 Structure	19
3.2 Biological function of CD73	20
3.2.1 Enzymatic activity	20
3.2.2 Enzyme-activity unrelated functions	21
3.3 Expression of CD73	22
3.3.1 Tissue distribution of CD73	22
3.3.2 Expression of CD73 on immune cells	23
3.4 Role of CD73 in human diseases	24
3.4.1 Calcification of joints and arteries	24
3.4.2 CD73 and cancer	24
3.5 Targeting of CD73	25
3.5.1 Monoclonal antibodies	25
3.5.2 Antibody mimetics	25
4 Objectives	26
5 Materials and methods	27
5.1 Materials, chemicals and instruments	27
5.1.1 Instruments	27
5.1.2 Chemicals and materials	28
5.1.3 Software	29
5.2 Molecular cloning	30

5.2.1	His-tagged recombinant human CD73 for mammalian expression system	30
5.2.2	Polymerase chain reaction	30
5.2.3	Agarose gel electrophoresis	30
5.2.4	Cleavage using restriction endonucleases	30
5.2.5	Ligation of DNA fragments	31
5.2.6	Heat shock transformation of <i>E. coli</i>	31
5.2.7	Minipreparation of plasmid DNA	32
5.2.8	Maxipreparation of plasmid DNA	32
5.2.9	DNA sequencing	32
5.3	Protein expression in mammalian system HEK293–6E	32
5.3.1	Small-scale transient transfection of HEK293–6E on a 6-well plate	32
5.3.2	Large-scale transient transfection of HEK293–6E in Erlenmeyer flasks	33
5.3.3	Harvesting of secreted protein	33
5.3.4	Affinity chromatography – purification using 6xHis-tag	33
5.3.5	Protein concentration measurement	34
5.4	SDS PAGE	34
5.5	Silver staining of SDS polyacrylamide gel	35
5.6	Western blot and immunodetection	35
5.7	Malachite Green Assay for CD73 activity measurement	35
5.8	DNA-linked Inhibitor Antibody Assay – DIANA	36
5.8.1	Preparation of oligonucleotide conjugate as probes for DIANA	37
5.8.2	Standard DIANA testing method	37
5.8.3	Optimisation of conditions	38
5.8.4	Determination of dissociation constant of probes	38
5.9	Enzyme-Linked Immunosorbent Assay – ELISA	39
5.10	Preparation of stable transfectants expressing CD73	39
5.11	Flow cytometry	39
6	Results	41
6.1	Molecular cloning	41
6.2	Small-scale transfection	41
6.3	Large-scale expression and purification of rhCD73	42
6.4	Inhibition constant measurement	44
6.5	DIANA	45
6.5.1	Probes preparation	45
6.5.2	Optimising of DIANA method for rhCD73	45
6.5.3	Determination of the dissociation constant of DIANA probe P4	47
6.5.4	High-throughput screening of IOCB library	47
6.6	Preparation and characterisation of anti-CD73 iBody	47
6.6.1	Anti-CD73 iBody preparation	47
6.6.2	Characterisation of interaction between anti-CD73 iBody and rhCD73 using ELISA	47
6.6.3	Flow cytometry measurement of binding of anti-CD73 iBody to cells	48

7	Discussion	50
8	Conclusion	54
	Appendix	55
	References	56
	List of Figures	67
	List of Tables	67

List of Abbreviations

AA	amino acid
AOPCP	also AMPCP, Adenosine 5'-(α , β -methylene)diphosphate
AP	acute pancreatitis
APS	ammonium persulfate
BiTE	bispecific T cell engager
CAF	cancer associated fibroblast
CALJA	calcification of joints and arteries
cAMP	cyclic AMP
CAR-T	chimeric antigen receptor engineered T cells
CD	cluster of differentiation
CD73	cluster of differentiation 73
CRE	cAMP response element
CRS	cytokine release syndrome
CTLA-4	cytotoxic T-lymphocyte-associated antigen 4
CV	column volume
DAMP	damage-associated molecular pattern
DC	dendritic cell
ELISA	Enzyme-Linked Immunosorbent Assay
EMT	epithelial to mesenchymal transition
EPR	enhanced permeability and retention effect
ER	endoplasmatic reticulum
FDA	Food and Drug Administration
GITR	glucocorticoid-induced TNF receptor family-related protein
GPI	glycosylphosphatidylinositol
HPD	hyperprogressive disease
HPMA	<i>N</i> -(2-Hydroxypropyl) methacrylamide
HPV	human papillomavirus
HRP	horseradish peroxidase

ICOS	inducible T cell co-stimulator
iNKT	invariant natural killer T cell
IOCB	Institute of Organic Chemistry and Biochemistry of the Czech Academy of Science
LAG-3	lymphocyte activation gene-3
IPEI	linear polyethylenimine
MHC I	major histocompatibility complex I
NAD	nicotinamide adenine dinucleotide
NK	natural killer
NMN	nicotinamide mononucleotide
PAMP	pathogen-associated molecular pattern
PCR	polymerase chain reaction
PD-1	programmed cell death protein 1
PD-L1	programmed cell death ligand 1
RLU	relative luminescence unit
sCD73	soluble CD73
TAM	tumour associated macrophage
TCR	T cell receptor
TEMED	tetramethylethylenediamine
TGF- β	transforming growth factor β
TIGIT	T cell immunoglobulin and ITIM domain
TIL	tumour-infiltrating lymphocyte
TIM-3	T cell immunoglobulin-3
TME	tumour microenvironment
VEGF	vascular endothelial growth factor
VISTA	V-domain Ig suppressor of T cell activation

Introduction

Cancer is one of the most common causes of death, in 2018 about 9.6 millions of people died due to cancer worldwide. There are plenty of treatment options, such as surgery, radiation and chemotherapy, but in the last decade, immunotherapy begins to take over. The classical approaches to cancer treatment exhibit serious side effects and do not go to the essence of the problem. Immunotherapy on the other hand is really costly and effective only in a subset of patients. There are several ways in which immunotherapy evolves rapidly and as the knowledge of tumour microenvironment grows, other therapeutically relevant pathways are revealed.

One of those pathways involved in tumour immune escape is purinergic signalling with two major ecto-enzymes CD39 and CD73, converting immune activator ATP to immunosuppressive adenosine. Higher levels of those enzymes in tumour microenvironment contribute to the immune escape and can be thus counted as immune checkpoints. CD73 is GPI anchored membrane protein over-expressed on cancer and immune cells present in the tumour. This 70kDa protein occurs in homodimer form on the cell surface. The enzymatic activity of CD73 produces immunosuppressive adenosine inhibiting cytotoxic T cells thus increasing the resistance to immunotherapy. It was also shown that CD73 contributes to cancer progression and therapy-resistance in non-enzymatic ways.

Developing new selective inhibitors can be one way how to modulate the tumour microenvironment and when attached to the polymer particle, it can be used for tumour targeting as well. Moreover, due to the EPR effect (enhanced permeability and retention effect) of the polymer, inhibitor will accumulate in the tumour, as it was shown for HPMA copolymers. The polymer conjugates labelled with fluorescence tag can be then used also for tumour imaging.

Several antibodies targeting CD73 are now in clinical trials and pharmaceutical companies focus on new small-molecules with inhibitory effect on CD73. This thesis describes inhibitor screening of small-molecule library and development of antibody mimetics targeting CD73 with CD73 inhibitor as targeting ligand, thus combining both highly-potent approaches to disable CD73 anti-inflammatory activity.

1 Cancer treatment overview

1.1 Classic approaches to cancer treatment

The primary method of cancer treatment is surgery. Solid tumour, surrounding tissues and in certain cases also lymph nodes are surgically removed if possible. Surgery is usually combined with radiation and or chemotherapy.

In chemotherapy, cytotoxic drugs are used, targeting rapidly dividing cells by interfering with mitosis [1]. Besides cancer cells, other rapidly dividing cells are affected by those anti-mitotics, manifesting in significant side effects such as alopecia, decreased production of blood cells and inflammation of digestive tract.

In radiation therapy, cancer cells are destroyed directly with ionising radiation. Side effects depend on the irradiated organ, doses of radiation and other factors – skin irritation usually occurs often along with fatigue and nausea.

1.2 Immune system

The primary role of immune system is to prevent pathogen infection. At the same time, the immune system is also responsible for disposal of ageing and damaged cells.

The immune system can be divided in two parts. First there is nonspecific innate immune system including macrophages, dendritic cells (DC), granulocytes (such as eosinophils, basophils, neutrophils and mast cells) and natural killers (NK). Secondly, there is the adaptive antigen-specific system, which consists of humoral and cellular immunity. The cellular immunity is ensured by T lymphocytes, while the humoral by antibody-producing B lymphocytes.

The innate system reacts to so-called PAMPs (pathogen-associated molecular patterns) or DAMPs (damage-associated molecular patterns) and the adaptive system is activated subsequently.

At the cellular level, there are two lineages of hematopoietic cells — myeloid and lymphoid (see Figure 1 on page 13). For further classification of leukocyte subpopulations, so-called CD nomenclature was established in 1982 [2]. Abbreviation CD stands for cluster of differentiation, pursuant to the clusters of monoclonal antibodies interacting with those molecules. There have been up to 371 CD molecules described up to April 2019 according to UniProt database [3].

A cancer cell can be viewed as a damaged cell with pathogenic behaviour. Therefore, there is no wonder that the immune system has the potential to dispose of it. The failure of the immune system to recognise or kill cancer cells results in tumour growth.

1.3 Immunotherapy

At present there is a wide variety of approaches to cancer treatment. The classical approaches have serious side effect with limited room for improvement. Immunotherapy based on boosting patient's own immunity has recently become very prominent.

The idea of immunotherapy is derived from the so-called cancer-immunity cycle. First, cancer antigens released from the tumour are captured by antigen presenting cells (APC) and delivered to the lymph nodes. In the lymph nodes, T cells can recognise the antigens presented by APCs. After receiving another

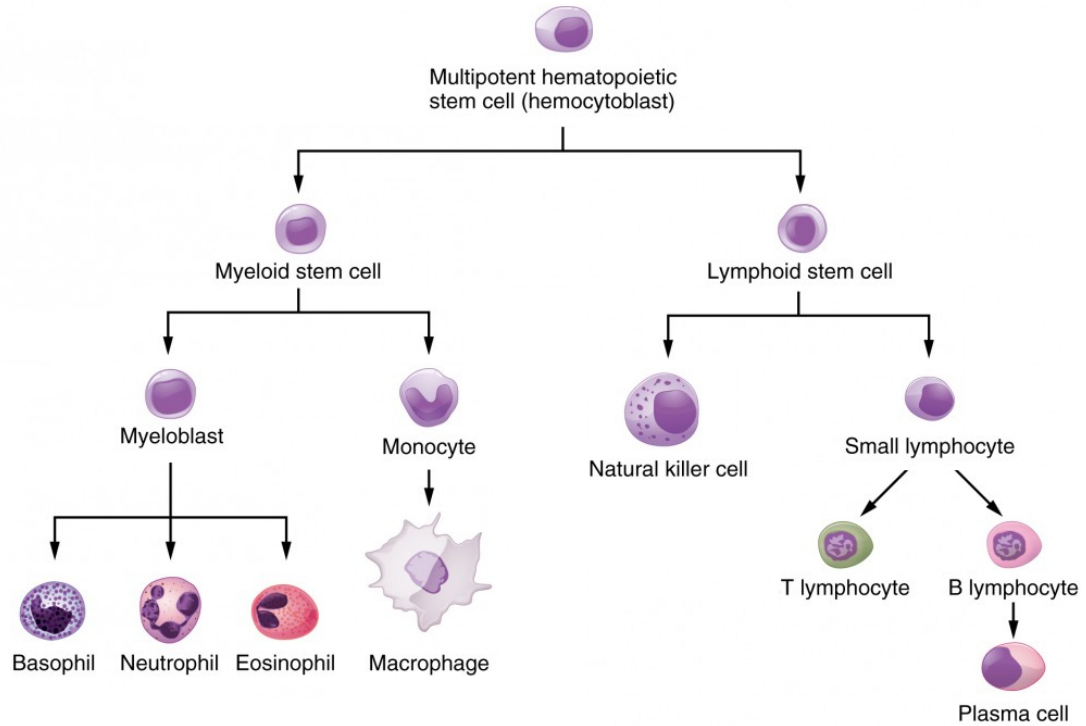


Figure 1: Overview of basic leukocyte types. Adapted from [4].

co-stimulatory signal, T cells become activated, start to proliferate, migrate to the tumour and kill the cancer cells. Dead cancer cells then serve as a source of the antigens [5].

Intervention during any step of this cycle can potentially be used for immunotherapy. Even before antigen release, vaccination is a powerful tool for preventing tumour growth. Using checkpoint inhibitors leads to T-lymphocyte priming and activation [6]. Additionally, bispecific T cell engagers (BiTE) were developed to recruit T cells for the specific killing of cancer cells.

The main goal of immunotherapy is to initialise or amplify cancer-immunity cycle without generating autoimmune inflammatory response. For this task it is important to find the rate-limiting step which varies among the patients and the types of tumours.

1.3.1 Vaccination

Historically, vaccination has proven to be successful approach in prevention of many infectious diseases. The development of anticancer vaccines is more challenging. Firstly, specific cancer antigens which are not present on normal cells have to be found. Furthermore, cancer cells evolve quickly in the process called immune editing [7] and create immunosuppressive tumour microenvironment that inactivates effector lymphocytes. Despite the challenges, this approach can be successful. More than ten years ago, a vaccine was developed against the most malignant subtypes of cancerogenic virus – human papillomavirus (HPV) [8]. The vaccine significantly decreases the incidence of cervical cancer in vaccinated subjects.

1.3.2 Adoptive T cell therapy

In adoptive T cell therapy, the main goal is to obtain anticancer immunity by *ex vivo* manipulated lymphocytes and then administer them back to the patient.

The first type of adoptive T cell therapy is tumour-infiltrating lymphocytes (TIL) therapy that can be used for treatment of solid tumours. In this approach, patient's own TILs are expanded *ex vivo* after being proven to recognise cancer cells. This therapy shows efficacy in many cancer types including melanoma, breast, colorectal and bile duct cancer (preliminary studies) [9–12].

Another way to obtain anti-cancer T cells is genetic manipulation of autologous T cells *in vitro*. One of the most promising approaches seems to be the transfection of patients' T cells with chimeric antigen receptor (CAR) against cancer surface antigen. This therapy has been already approved by Food and Drug Administration (FDA) in 2017 and works well especially for treatment of B cell malignancies [13]. Currently, two CAR-T therapies have been FDA approved [14] – KYMRIAH® (Novartis) against acute lymphoblastic leukemia and YESCARTA® (Gilead) against certain types of non-Hodgkin's lymphoma.

Another approach is to engineer high-affinity T cell receptor (TCR) with enhanced tumour-recognition ability. The main difference between CAR-T and affinity-enhanced TCR is that CAR-T can recognise surface tumour antigens while TCR recognise tumour-specific fragments from the inside of the cell presented on the MHC I (major histocompatibility complex I).

Side effects of adoptive T cell therapies are mostly cytokine release syndrome (CRS) [15], low blood pressure and weakened immune system. Neurotoxicity and other changes in the brain was observed in some patients [16]. However, recently new CAR-T drugs were developed with no serious observed side effects [17].

1.3.3 Bispecific T cell engager

For T cell activation, bispecific antibodies (bispecific T cell engager, BiTE) were developed. BiTE consists of two single-chain variable fragments (scFv) linked together. One scFv targets the CD3 receptor on T cell, the other scFv targets a cancer antigen [18]. T cell becomes activated through the interaction with CD3 and can destroy neighbouring cancer cells by the release of cytotoxic granules. The first BiTE therapy was approved for acute lymphoblastic leukemia via CD19 targeting by FDA in 2014 [19].

1.3.4 Oncolytic viruses

Another cancer-antigen driven approach is to use oncolytic viruses that are targeted directly to the tumour. After the infection, virus destroys the cancer cells, which leads to additional release of tumour antigens and activation of the immune system [20]. The immune response is also amplified via release of viral antigens [21].

In the process of tumourigenesis, most of the cells lose their innate ability of antiviral response, which facilitates oncolytic therapy [22]. Beside direct injection of virus into the tumour, other approaches of delivery are being studied such as use of infected tumour-infiltrating lymphocytes.

The first oncolytic therapy of melanoma used modified *Herpes simplex* virus lacking genes responsible for its virulence but containing gene for stimulating factor GM-CSF [23]. At present, various virus families are being tested, such as

adenovirus, herpesvirus, poxvirus, paramyxovirus, reovirus, rhabdovirus, picornavirus and parvovirus [22, 24].

1.3.5 Checkpoint inhibitors

There is a fragile balance between stimulation and suppression of immune system. The balance is guarded by the immune checkpoints therefore, in many cases, the antigen exposure is not sufficient for the T cell activation. The final response is determined by the number of activatory and inhibitory signals. Cancer cells can manipulate the immune response by overexpression of these inhibitory immune checkpoints.

One of the checkpoints is T cell immunosuppressive interaction of cytotoxic T lymphocyte associated antigen 4 (CTLA-4) [25] and its ligands CD80 and CD86. This interaction occurs in lymphoid organs and could be disrupted by anti-CTLA-4 antibodies and thus enabling autoreactive T cells to emerge [26, 27].

The effector phase of activated T cell in (cancer) tissue is inhibited by interaction of programmed cell death protein 1 (PD-1) present on the surface of T cell with programmed death ligand 1 (PD-L1) overexpressed in cancer cell and tumour-infiltrating leukocytes [28]. Blockade of this interaction leads to antitumour activity by releasing the breaks of the immune system [29].

Discovery of these two pathways had significant impact on cancer immunotherapy and lead to Nobel Price awarded jointly to James P. Allison and Tasuku Honjo for Physiology and Medicine in 2018. There are currently (as of March 2019) seven immune checkpoint inhibitors approved by FDA.

Recently, new immune checkpoint inhibitory pathways were discovered, such as lymphocyte activation gene-3 (LAG-3), T cell immunoglobulin-3 (TIM-3), T cell immunoglobulin and ITIM domain (TIGIT) [30] on NK and T cells. Under investigation are also stimulatory pathways including glucocorticoid-induced TNF receptor family-related protein (GITR), inducible co-stimulator (ICOS) and CD40. There is also V-domain Ig suppressor of T cell activation (VISTA), known as programmed death-1 homolog (PD-1H), serving as stimulatory signal for APC, but inhibitory for T cells [31].

2 Tumour microenvironment

In many cases (immuno)therapy does not have the desired therapeutic effect. Furthermore, it sometimes leads to accelerated tumour growth [33]. Mechanism of this so-called hyperprogressive disease (HPD) still remains uncertain but several hypotheses have been proposed [34].

Both ineffective therapy and HPD can be explained by changes of the tissue in and around the tumour. These changes during tumorigenesis result in establishment of so-called tumour microenvironment (TME) which includes both cellular and non-cellular components [35]. To overcome drug resistance, targeting different TME components could be beneficial. Targeting non-tumour cells seems to be more advantageous due to their genetic stability [36].

Besides malignant cells, the TME contains cancer associated fibroblasts (CAF), endothelial cells and neovasculature-forming pericytes, cells derived from bone marrow, stromal cells and immune cells [36]. The extracellular matrix is part of TME as well.

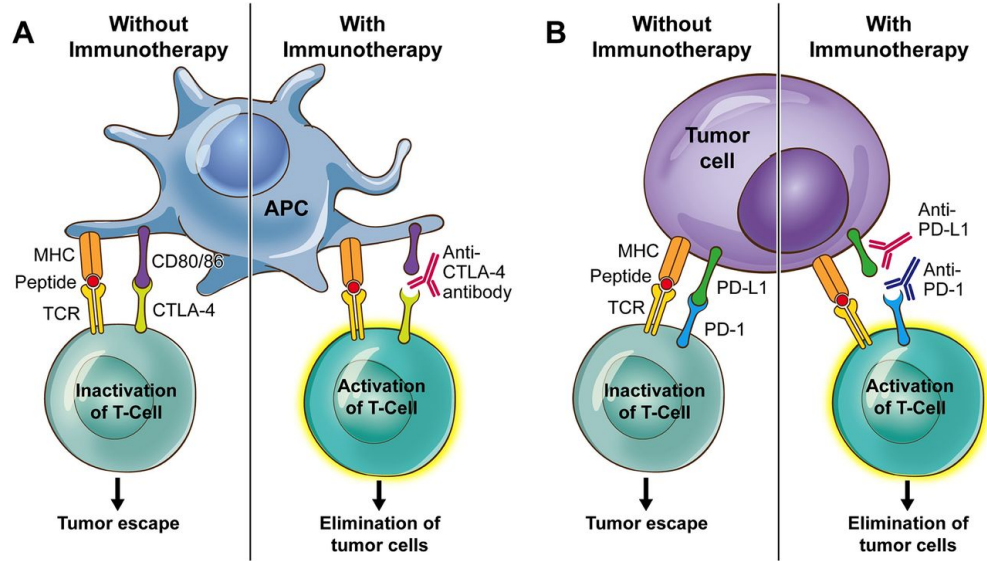


Figure 2: Role of immune checkpoint inhibitors in T cell activation. **A)** cytotoxic T-lymphocyte-associated protein-4 (CTLA-4); **B)** programmed death-1 (PD-1). Adapted from Soularue et al. [32].

2.1 Cancer associated fibroblasts

Activated fibroblasts that promote tumour progression are called cancer associated fibroblasts (CAF). Unlike normal fibroblasts, CAFs do not return to normal phenotype after activation and do not undergo apoptosis [37].

Main role of CAFs in tumour is stimulation of angiogenesis and cell proliferation by cytokine and growth factor production, such as vascular endothelial growth factor (VEGF) and transforming growth factor β (TGF- β). Another important role is regulating immune response by expression of immunosuppressive receptors, PD-L1 and PD-L2 [38] and also CD73 [39]. Furthermore, they can affect stiffness of extracellular matrix thus enable spreading the tumour to the neighbouring tissue.

2.2 Immune cells in tumour microenvironment

Despite the primary role of the immune system to recognise pathogens and damaged cells and destroy them, the migration of immune cells into the tumour often causes its progression. While the TME contains all types of immune cells, the composition differs from healthy tissue. Moreover, some immune cells even promote tumour growth.

Signs of chronic inflammation can be observed in the tumour, marked by release of immunosuppressive growth factors (TGF- β , IL-10). These growth factors drive immune response towards regulatory one without cytotoxic activity [40]

One of the typical leukocyte type present in tumour is tumour associated macrophage (TAM) – type M2 macrophage [41]. TAMs concentrate in hypoxic regions of tumour contributing besides CAFs to angiogenesis due to VEGF signalling [42].

The major impact of TAMs is the production of various cytokines that suppress cytotoxic T cells as well as directly inhibiting them by ligands of PD-1 and CTLA-4. CD73 is also expressed in TAMs. The expression of immune checkpoints prevents T cell cytotoxicity and promotes apoptosis in cytotoxic T cells.

Additionally, chemokines produced by TAMs are attracting Tregs (regulatory T cells) thus suppressing cytotoxic T cells in another manner [43].

2.3 Purinergic signalling

Purinergic signalling plays an important role in the regulation of the immune system. In phylogenesis, both immunosuppressive and activation signalling cascades have evolved. An inappropriate response can enable massive bacterial infection on the one hand, on the other hand can cause damage to its own tissues. One common pathway, called purinergic signalling, uses signalling by purine nucleotides and nucleosides, such as ATP, AMP and adenosine. This signalling cascade belongs to the most important immunosuppressive signalling in the TME.

First, cells release ATP – a strong activator of immune system – into the extracellular space. Second, ATP is converted by membrane-bound enzymes in several steps to adenosine – a strong immunosuppressant [44].

2.3.1 Mechanism of ATP release

The most common way of ATP release to extracellular space is directly from damaged cell with broken membrane. There are several other ways of specific ATP transport – facilitated diffusion with nucleotide transporters, vesicular exocytosis and transport through channels that could be activated under different conditions [45].

2.3.2 Enzymes involved in purinergic signalling

The ATP breakdown to adenosine is ensured by ectonucleotidases, alkaline phosphatases, pyrophosphatases and phosphodiesterases [46]. The well-studied pathway begins with CD39 converting ATP to AMP and in the next step CD73 dephosphorylates AMP to adenosine. Alternatively, AMP can be generated from NAD⁺ by CD38 cleavage [47].

The standard concentration of extracellular ATP in normal tissue is in nanomolar range whereas in solid tumours the concentration is approximately 10000 times higher – hundreds of micromolar [48]. This enormous amount of ATP is being converted to adenosine by the enzymatic activity of the purinergic pathway [49] and causes a huge immunosuppressive response by activating both high-affinity and low-affinity adenosine receptors.

2.3.3 Purine receptors

In every signalling pathway, receptors for signal molecules are crucial. Receptors for purines are classified in two categories – P1 and P2. Adenosine activates P1 receptors and ATP activates P2 receptors that are further divided in two subcategories P2Y and P2X [50]. Receptors P1 and P2Y belong to G-protein coupled receptor family while P2X are ligand-gated ion channels. So far, four P1 adenosine receptors (sometimes abbreviated AR) – A₁, A_{2A}, A_{2B}, A₃ – and for ATP seven P2X and eight P2Y are known [48]. The overview of purine receptors is depicted in Figure 3 on page 18.

Purine receptors differ in ligand specificity, their intracellular signalling cascade and presence on the surface of different cell types. For instance, P2X recognise only ATP, but some of P2Y receptors can be activated by other nucleotides (ADP, UTP, UDP, NADP) [52]. Lymphoid lineage expresses only P2X receptors,

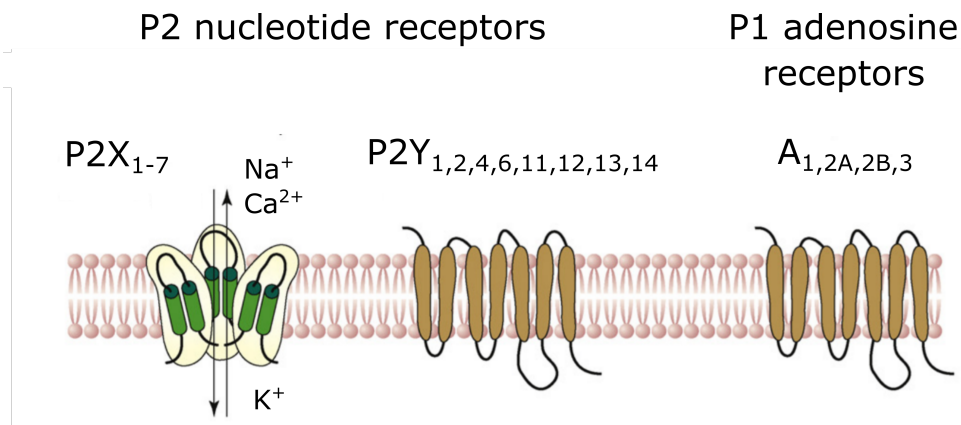


Figure 3: Overview of purine receptors – adenosine receptors P1 and nucleotide receptors P2. Adapted and modified from Abbracchio et al. [51].

while myeloids, such as dendritic cells (DC) and monocytes, are expressing both P2X and P2Y [48].

The activation of immune system by ATP on molecular level leads to chemotaxis (macrophages, DC), inhibition of immunosuppressive cytokine synthesis (IL-12) and activation of pro-inflammatory cytokines like IL-10 [53]. ATP-mediated activation is visible at both CD4⁺ and CD8⁺ T cells [48] and iNKT cells (invariant natural killer T cells) [54].

Above that, purinergic signalling is also involved in pain nociception. ATP released from injured tissue mediates pain in peripheral nerves [55] and adenosine induces analgesia [56]. Thus CD73 is potential therapeutic target in chronic pain mitigation.

3 Ecto-5'-nucleotidase

CD73 is ecto-5'-nucleotidase (NT5E; EC 3.1.3.5). It is a member of the superfamily of metallo-phosphoesterases [57]. This enzyme is also known as 5'-ribonucleotide phosphohydrolase or CALJA (Calcification of joints and arteries) and is encoded by the gene *NT5E*. Protein naturally occurs in homodimer form of two approximately 70kDa subunits anchored by GPI (glycosylphosphatidylinositol) to plasma membrane. Those monomers are not bound together by disulfidic bridges but only by non-covalent interactions [58].

In addition to the membrane-bound CD73, the soluble form of CD73 (sCD73) is present in plasma [46, 59]. The GPI anchor is cleaved by phosphatidylinositol-specific phospholipase and the sCD73 is released. Increased concentration of sCD73 often correlates with a severity of several diseases as well as poor prognosis. This was proven for e.g. acute pancreatitis (AP) [60], sickle cell disease [61] and cancer [62, 63]. Thus sCD73 in plasma is a good marker for diagnosis and treatment process and also a good prognostic marker due to the easy concentration determination [63]. Besides plasma, sCD73 was also found in the lymph [64].

Except for ecto-5'-nucleotidase there is cytosolic homolog – cytosolic 5'-nucleotidase – that is not structurally similar [65]. Another CD73 homolog is bacterial 5NT with analogous enzymatic activity and structure yet displaying several differences. Unlike human CD73, the bacterial one is monomeric and does not

exhibit the same enzymatic specificity [57, 66].

3.1 Structure

In 1999, the first structure of bacterial CD73 was published [66], giving an insight into basic properties of this enzyme family. Few years later the structure of CD73 from *Candida albicans* [67] was elucidated. It turned out that this eucaryotic CD73 was less related to the human than the bacterial one. Currently, the crystal structures of human CD73 are available with 1.55-2.0 Å resolution and in complex with several ligands [68, 69].

The enzyme consists of two domains – bigger N-terminal domain contains ion binding site and the smaller C-terminal domain contains substrate binding site and dimerisation interface. Both domains are linked by short α -helix, so called hinge region. This helix ensures flexibility thus enabling the enzyme to switch from open to closed conformation and back (see Figure 4 on page 19).

The enzyme is synthesised in propeptide form and subsequently undergoes posttranslational modifications. Whole length of CD73 before cleavage is 574 amino acids (AA). Because of the localisation on the extracellular side of the plasma membrane, the secretory signal peptide (1 – 26 AA) on N-terminus delivers the enzyme into the endoplasmatic reticulum (ER), then it is cleaved off. In the ER, the GPI anchor – synthesised directly in the ER vesicle [70] – replaces the C-terminal propeptide sequence (550 – 574 AA). The GPI anchor is a hydrophobic moiety made up of a lipid-modified phosphatidylinositol [71]. In the mature form, CD73 has five disulfide bridges between cysteins and four N-glycosylations on asparagines.

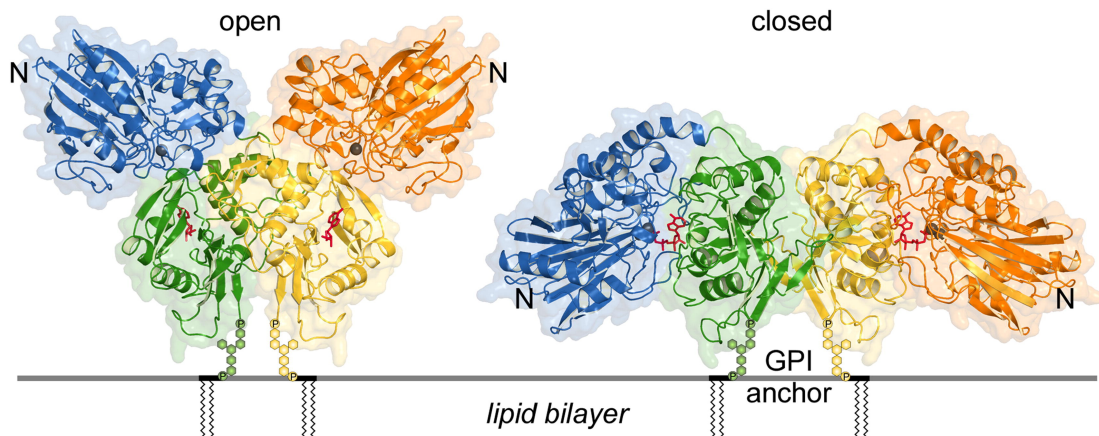


Figure 4: Structure of CD73 in open and closed conformation.

One subunit of CD73 dimer is depicted in blue and green, the other in orange and yellow. Blue and orange are N-terminal domains, green and yellow C-terminal. Ligands are shown as red sticks and ions as grey spheres. Connection to membrane by GPI anchor is shown schematically. Adapted from Knapp et al. [68].

The active site is formed by both N-terminal and C-terminal domains in the closed conformation. Substrate is first bound in the open conformation far away from the ion binding site and the binding then induces the N-terminal subunit movement resulting in the closed state. That involves massive water exclusion

from the protein surface and the substrate pocket also remains water inaccessible after closure [68].

The substrate binding in the active site is ensured by hydrogen bonds mediated by water molecules and also via strong hydrophobic π -stacking. The active site contains two zinc ions necessary for the activity. The structure of the active site with noncleavable substrate analog AOPCP (adenosine 5'-(α,β -methylene)diphosphate) – well-known inhibitor of CD73 – is depicted (see Figure 5 on page 20).

The structures of CD73 with different ions in the active site such as Co^{2+} and Mn^{2+} were published [72–74].

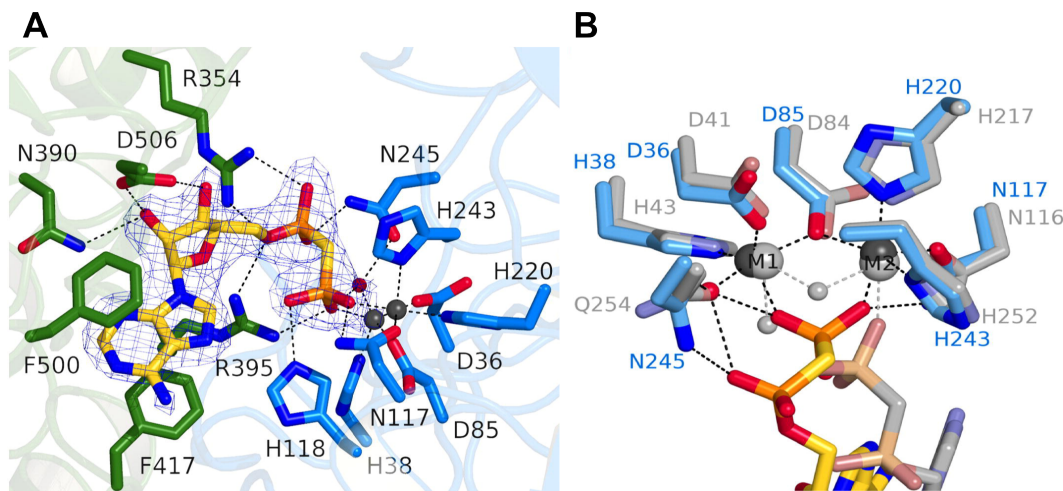


Figure 5: Structure of active site of CD73 with AOPCP.

A) Active site in closed conformation with bound inhibitor AOPCP. The two zinc ions are shown as grey spheres. **B)** Comparison of the binding modes of the terminal phosphonate groups of AOPCP to the zinc ions of human CD73 (bright colours) and *E. coli* homolog of CD73 (grey and dim colours). Adapted from Knapp et al. [68].

3.2 Biological function of CD73

There are many biological functions of CD73, both related and unrelated to its enzymatic activity. Previously, it was thought that all functions are related to the enzymatic activity, but later series of experiments revealed other functions of CD73. To distinguish between these two roles of CD73, comparison between CD73 knock-down cells and cells with inhibited CD73 activity were studied. For melanoma was shown that not only enzymatic activity is important for its invasiveness [75].

3.2.1 Enzymatic activity

The main function of CD73 is its enzymatic activity. This ectonucleotidase is able to dephosphorylate various ribonucleotides with strong preference for AMP. The phosphonate group of ribonucleoside 5'-phosphate (AMP) is hydrolysed in the presence of bivalent metal ions (Zn^{2+}). The products of the reaction is ribonucleoside (adenosine) and one equivalent of phosphate.

Besides AMP, CD73 cleaves NAD (nicotinamide adenine dinucleotide) and NMN (nicotinamide mononucleotide) [76].

3.2.1.1 Inhibitors

Unlike bacterial NT5E capable of AMP, ADP and ATP cleavage, human CD73 is only able to cleave ribonucleotide monophosphates while di- and tri- phosphates, like ADP and ATP, are natural CD73 inhibitors [46].

Many CD73 competitive inhibitors are derived from substrate scaffold with substitution of the phosphate for noncleavable phosphonomethyl. The first synthetic inhibitor is AOPCP (adenosine 5'-(α , β -methylene)diphosphate) [77]. A series of highly potent inhibitors derived from AOPCP was published in 2015, with the most potent inhibitor PSB12379 (*N*⁶-benzyl-adenosine-5'-*O*-[(phosphonomethyl) phosphonic acid]) with K_i in single nanomolar digits [78].

Not all inhibitors of CD73 are derived from AMP. They can be divided in three main categories – quercetin-based flavonoids [79], molecules with anthraquinone scaffold [80] and sulfonamides [81]. Pharmaceutical companies, such as Arcus Biosciences, have a small-molecule program for CD73 inhibitor search [82].

Beside small organic compounds, many inhibitory antibodies with therapeutic effect were found as well [83, 84]. For further details see Section 3.5.

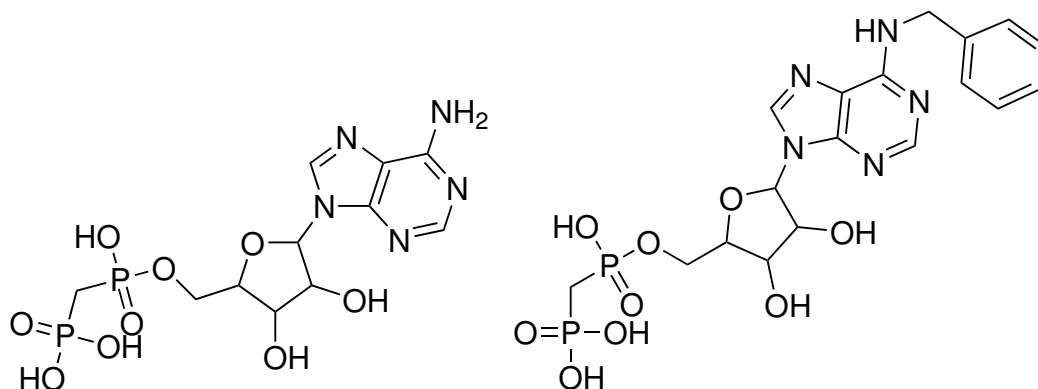


Figure 6: Competitive inhibitors of CD73. On the left is the well-known inhibitor AOPCP, on the right highly potent inhibitor PSB12379, $K_i = 2.21$ nM (rhCD73) according to Bhattarai et al. [78].

3.2.2 Enzyme-activity unrelated functions

The non-enzymatic role resides in participation of CD73 in cell migration and adhesion. The CD73 exhibits receptor-like character by interaction with glycoproteins in extracellular matrix such as tenascin C, which significantly regulates activity of focal adhesion kinase (FAK), thus influencing cell mobility.

In the case of breast cancer, overexpressed CD73 promotes cancer cell mobility and adhesion to extracellular matrix [85]. It was previously shown that expression of CD73 enhances lymphocyte binding to the endothelium [86].

Furthermore, CD73 plays co-stimulatory role in activation of cytotoxic CD8⁺ T cells [87, 88].

3.3 Expression of CD73

CD73 is encoded by the gene *NT5E* located on chromosome 6 locus q14.3 and it undergoes several modifications after translation – signal sequence cleavage, GPI anchor attachment, four N-glycosylations and five disulfide bridges forming – resulting in approximately 70kDa protein attached to the plasma membrane by GPI anchor. Tissue distribution of CD73 both on mRNA and protein level was characterised several times in different projects – The Genotype-Tissue Expression project (GTEx) [89, 90], FANTOM5 Consortium [91] and Human Protein Atlas (HPA) [92, 93].

Several splice variants of *NT5E* gene exist, but so far, their role remains elusive. There are some reports about one isoform of CD73 (CD73S) lacking 49 AA (404–453) [94]. This isoform was found to be upregulated in cirrhosis and hepatocellular carcinoma, but not in healthy liver tissue. This shorter variant CD73S lacks enzymatic activity, can not form a dimer, but is involved in regulation of degradation of canonical CD73 in the liver [95].

3.3.1 Tissue distribution of CD73

CD73 is expressed in several tissues, mainly those forming barriers such as endometrium, vasculature, colon, kidney, liver, lung and also in other tissues like brain, muscles and retina. As the "cluster of differentiation" name implies, CD73 is expressed on leukocytes – subset of B and T lymphocytes and also myeloid cells such as neutrophils and macrophages.

Highest expression of CD73 in normal tissue, both on protein and mRNA level, was found in female tissues such as cervix, uterus and endometrium [89, 91, 92]. CD73 is highly expressed in vascular endothelium where it helps seal interendothelial gaps by released adenosine. This role is important for closing of widened junctions after leukocyte migration through the tissue [96].

Expression of CD73 also strongly correlates with the ion transport capabilities of the tissue. The expression of CD73 in the mucous epithelial tissue is polarised and is present only on apical surface [97] suggesting that CD73 plays important role also in ion transport. It is not known how CD73 affects ion transport [96].

In general, CD73 is guarding all tissue barriers, both endothelial and epithelial [98]. In CD73 knock-down mouse, it was shown that CD73 expression is induced by hypoxia-inducible factor (HIF) which is crucial for preventing vascular permeability during hypoxia [96, 99, 100].

Expression of CD73 is negatively regulated by estrogen and also androgen receptor as it was shown for nine breast cancer cell lines and two prostate cancer cell lines, respectively. The breast cancer cell lines lacking estrogen receptors exhibit more than 100-fold CD73 activity. The increased expression correlates with aggressiveness of the tumour [101].

Extracellular adenosine, produced by CD73, elevates production of cAMP (cyclic AMP) through the interaction with adenosine receptor that subsequently downregulates the transcription of *NT5E* gene. Promotor of that gene contains cAMP response element (CRE), ensuring negative feedback of CD73 product [96, 102].

3.3.2 Expression of CD73 on immune cells

Cluster of differentiation 73 is present on a number of immune cells and is used as a marker of lymphocyte maturation [103]. CD73 is present both on myeloid and lymphoid leukocytes and on follicular dendritic cells derived from mesenchyme [104]. In general, CD73 is widely expressed on the subset of immunosuppressive leukocytes, inhibiting the pro-inflammatory activity.

In myeloid cells is CD73 expressed in neutrophils, which forms the crucial part of innate immunity, and provides them self-regulatory mechanism. Downregulation of CD73 in neutrophils causes their uncontrolled activation and elevation of adhesion to the vascular endothelium [105]. In macrophages, CD73 is expressed only in anti-inflammatory M2 macrophages, but not pro-inflammatory M1 [106]. In non-small cell lung cancer patients, upregulation of CD73 on myeloid-derived suppressor cells (MDSC) is detectable upon TGF- β stimulation.

Unlike in case of myeloid lineage, situation is different in case of lymphoid lineage of leukocytes. The main regulatory lymphoid cell is regulatory T cell (Treg), the CD39 was observed on its surface but surprisingly no CD73. Further investigation revealed that the observed immunosuppressive effect of Tregs is due to the expression of soluble sCD73 in the plasma [107]. The released adenosine then suppresses effector T cells [49]. CD73 is also expressed in Th17 helper cells, differentiated from naive T cells upon stimulation by IL-6 and TGF- β [108]. Cytotoxic CD8⁺ T cells have CD73 on their surface only in naive state. After their activation, CD73 is downregulated, in contrast to CD39 [109, 110].

On the B cells, CD73 is expressed mainly on memory Bmem cells, regulatory Bregs and subset of B1 cells [111–113]. Expression of CD73 in natural killers (NK) does not exceed 1 % of population, but when cocultured with mesenchymal stem cells, the expression of CD73 significantly grows [114]. Expression of CD73 on follicular dendritic cells mediates regulation of B cells maturation through adhesion to them in the lymphoid tissue [115, 116]. The overview of cells expressing CD73 is depicted in Figure 7 on page 23.

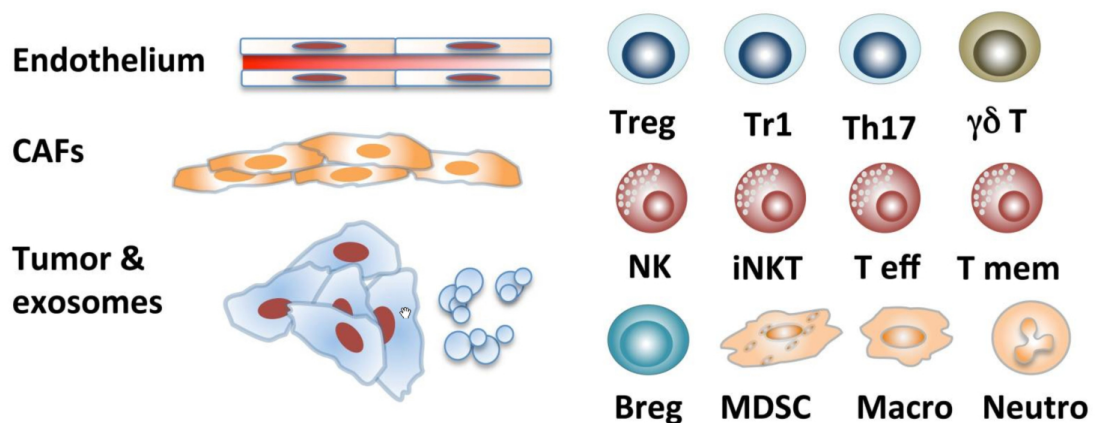


Figure 7: Overview of cells expressing CD73. Adapted and modified from Allard et al. [48].

3.4 Role of CD73 in human diseases

Several diseases have been described to be caused by protein alteration (calcification of joints and arteries) or changes in expression (cancer).

3.4.1 Calcification of joints and arteries

There is one disease known which is associated with the mutation in *NT5E* gene called CALJA – calcification of joints and arteries. The disease manifests in second decade of life usually with calcification of arteries and hand and foot joint capsules [117]. Several families with different point mutations of *NT5E* have been studied [118], the most common mutation is p.C358Y. Both nonsense and missense mutations result in reduced trafficking to the plasma membrane and the loss of enzyme function [118].

3.4.2 CD73 and cancer

CD73 was found to be upregulated in glioblastoma, melanoma, carcinomas of the colon, gallbladder, pancreas, ovary, breast and its metastases, lymph node metastases of prostate and others [119–124]. In most cases, CD73 upregulation correlates with poor prognosis of the patients and immunotherapy resistance. But CD73 may vary in its role in different types of cancer. Expression level of CD73 also differs in tumour stages of one type of tumour and changes in time. Because the CD73 transcription is induced by HIF, higher expression of CD73 can be found in hypoxic tumours [125]. Adoptive T cell immunotherapy and anti-PD-1 immunotherapy can cause CD73 upregulation in some patients [126], cytotoxic stress during chemotherapy can elevate CD73 levels as well [127]. Adenosine generated in the tissue often promotes aggressiveness and tumour growth, epithelial to mesenchymal transition (EMT), migration and invasiveness.

In the case of endometrial carcinoma, the role of CD73 is initially different. In early stages, the loss of CD73 activity, linked with reduced epithelial integrity, increases migration and invasion and facilitates metastases [128]. In later stages, the role of CD73 is similar to other cancer types.

Despite the fact that both endometrium and breast tissue are regulated by estrogen signalling, cancer of these tissues manifests in different manner, because the role of CD73 is different. In normal breast tissue, CD73 is expressed mostly in myoepithelial cells [129]. That correlates with the high aggressiveness of the triple negative breast cancer, subtype of breast cancer derived from myoepithelial cells [122]. However, it is still not clear, whether CD73 expression in breast cancer is sign of poor prognosis, as it is stated in [130], or good, as in [131].

3.5 Targeting of CD73

3.5.1 Monoclonal antibodies

Monoclonal antibodies (mAbs) are widely used for CD73 targeting [83, 121, 132, 133] and therapeutic potential of CD73 targeting has been shown in several preclinical studies. Two mAbs inhibiting CD73 activity are undergoing clinical trials. First of them, BMS-986179 is based on combination of IgG2 and IgG1 [134], the other MEDI9447 is based on IgG1 and targets active site of CD73 [133]. Both of them cause internalisation of CD73 upon binding thus eliminating both enzymatic and non-enzymatic activity.

3.5.2 Antibody mimetics

Antibodies are widely used for research, diagnostic and therapeutic purposes. Due to their costly production and biochemical instability, new synthetic alternatives are under investigation.

Synthetic polymer conjugates called iBodies were developed at the Institute of Organic Chemistry and Biochemistry with collaboration with Institute of Macromolecular Chemistry [135]. These antibody mimetics are based on HPMA (*N*-(2-Hydroxypropyl) methacrylamide) polymers that are water-soluble and biocompatible [136]. Due to reactive groups on the HPMA precursor, different ligands can be covalently attached [137]. Use of iBodies instead of antibodies in different biochemical assays has been evaluated previously [135]. In this thesis, three kinds of functional moieties have been attached to HPMA – inhibitor of CD73, fluorophore Atto488 and biotin (see Figure 8 on page 25). Due to the fluorescence tag Atto488, it is possible to visualise iBody, e.g. on flow cytometry, confocal microscopy and western blots. Biotin can be then used for immobilisation of the iBody through its interaction with NeutrAvidin in assays such as pull-down, SPR, ELISA and others.

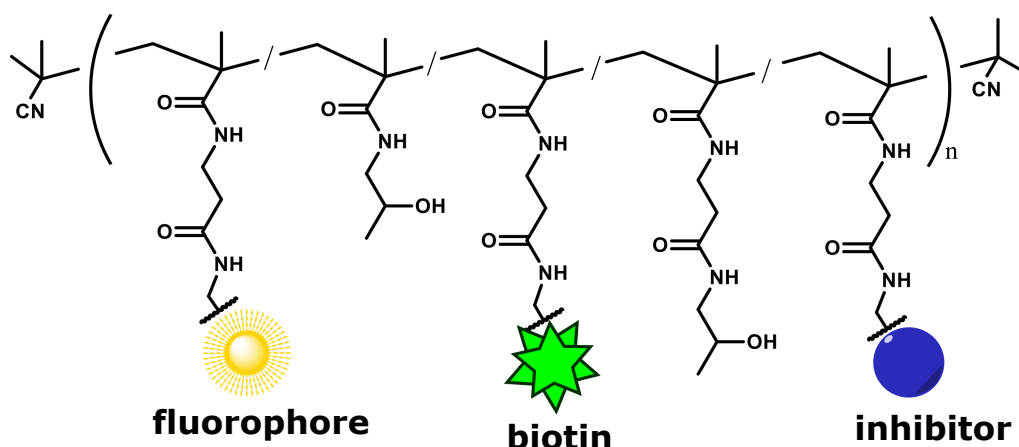


Figure 8: Schematic structure of HPMA copolymer decorated with functional molecules. Adapted from Sacha et al. [135].

4 Objectives

- Preparation of recombinant human CD73 (rhCD73) in a mammalian expression system.
- Purification of rhCD73 using affinity chromatography via His-tag.
- Optimisation of DIANA method for high-throughput screening of IOCB library¹ for a ligand of CD73.
- Preparation of polymer conjugate decorated with CD73 inhibitor called anti-CD73 iBody.
- Preparation of stable clones expressing membrane-bound CD73.
- Characterisation of prepared anti-CD73 iBody and its interaction with rhCD73 and with cell transfectants.

¹Small molecules prepared at IOCB Prague.

5 Materials and methods

5.1 Materials, chemicals and instruments

5.1.1 Instruments

- BD LSR Fortessa[™] cell analyzer, Becton, Dickinson and Company (USA)
- BlueWasher, Blue Cat Bio (Germany)
- Centrifuges:
 - Allegra X-15R, Beckman Coulter (USA)
 - Biofuge Pico, Heraeus Instruments (Germany)
 - Sorvall Evolution RC, Thermo Fisher Scientific (USA)
 - Microcentrifuge 5415R, Eppendorf (Germany)
- ChemiDoc-It 600 Imaging System, UVP (Germany)
- Countess cell counter, Thermo Fisher Scientific (USA)
- Horizontal electrophoresis apparatus, Gibco (USA)
- Infinite Reader M1000 PRO, Tecan (Switzerland)
- Incubator IPP 400, Memmert (USA)
- Laminary box: BSB4A Laminar Flow Box, Gelaire (Australia)
- LightCycler[®] 480 Instrument II, Roche Life Science (Germany)
- pH meter model pH 50, XS Instruments (Italy)
- Mini Trans-Blot cell, Bio-rad (USA)
- MP-500V power supply, Major Science (USA)
- Nanodrop ND-1000 spectrophotometer, Thermo Fisher Scientific (USA)
- Odyssey CLx Infrared Imaging System, LI-COR Biosciences (USA)
- Owl[™] EasyCast[™] B1A Mini Gel Electrophoresis Systems, Thermo Fisher Scientific (USA)
- Rotary shaker Innova 44, Eppendorf (Germany)
- ThermoCell Mixing block, BIOER (China)
- Trio 48 Thermocycler, Biometra (Germany)
- Vertical Apparatus – PAGE, Bio-Rad (USA)
- Voltage source EPS 301, GE Healthcare (USA)
- Water bath, Grant Instruments Ltd. (UK)

5.1.2 Chemicals and materials

- **Biotika** (Slovak Republic)
ampicillin
- **Bio-Rad** (USA)
All blue marker, Bradford solution
- **Biotium** (USA)
GelRed
- **Clontech** (USA)
Hygromycin B
- **Durocher, Yves** (Canada)
cell line HEK 293-6E, expression plasmid pTT28
- **Gibco** (USA)
L-glutamin, OPTIMEM, FreeStyle™ 293 Expression Medium
- **Lach-Ner** (Czech Republic)
ethanol, isopropanol, silver nitrate
- **Millipore** (USA)
Amicon Centrifugal filter units (MWCO 10000, 30000) 0.5, 4, 15 ml
- **New England Biolabs** (USA)
restriction endonucleases NheI and BamHI, T4 DNA ligase, 10x T4 DNA Ligase Reaction buffer, Phusion HF DNA polymerase, 5x Phusion HF Buffer, NEBuffer
- **Penta** (Czech Republic)
glycerol, acetic acid, sodium chloride, hydrochloric acid, sodium acetate
- **Polysciences** (USA)
IPEI 25 kDa
- **Promega** (USA)
Tris base
- **Qiagen** (Germany)
GelPilot DNA molecular weight marker, QIAquick Gel Extraction Kit, QIAquick PCR Purification Kit, Ni-NTA Superflow
- **R&D Systems** (USA)
Malachite Green Phosphate Detection Kit, PSB12379
- **SDT** (Germany)
Casein buffer 20×-4× concentrate
- **Serva** (Germany)
BSA, agarose

- **Sigma-Aldrich** (USA)
acrylamide, APS, bromophenol blue, cOmplete[™] His-Tag Purification Resin, dimethyl sulfoxide, glycine, EDTA, IMDM, imidazole, kanamycin, LB Broth, 2-mercaptoethanol, Pluronic F-68, SDS, sodium phosphate dibasic heptahydrate, potassium dihydrogen phosphate dihydrate, TEMED, Tween-20, sodium ascorbate, *N,N'*-Methylenebisacrylamide
- **SinoBiological** (P. R. China)
plasmid pCMV-N-Flag-NT5E, Anti-CD73 Antibody (PE)
- **Thermo Fisher Scientific** (USA)
NeutrAvidin, NeutrAvidin-HRP, Nunc 96-well plate Maxisorb (black), Nunc 96-well plate (transparent), polypropylene 5ml column, nitrocellulose membrane
- **Top-Bio** (Czech republic)
PCR dNTP mix
- **Zymo Research** (USA)
Zyppy[™] Plasmid Miniprep Kit, Zyppy Plasmid Maxiprep Kit
- **4titude** (UK)
FrameStar[®] 96-Well Semi-Skirted PCR Plate, adhesive plate seals

5.1.3 Software

- BD FACSDIVA[™], Becton, Dickinson and Company, (USA)
- ChemDraw[™] Professional, 16.0.1.4, PerkinElmer (USA)
- FlowJo[®] 10, Becton, Dickinson and Company, (USA)
- Image Studio[™], Biosciences (USA)
- Infinite M1000 PRO, Tecan (Switzerland)
- LightCycler[®] 480, Roche Life Science (Germany)
- Overleaf, online L^AT_EX Editor
- Prism 8.0.1, GraphPad (USA)
- VectorNTI, Thermo Fisher Scientific (USA)

5.2 Molecular cloning

5.2.1 His-tagged recombinant human CD73 for mammalian expression system

For expression in mammalian system HEK293–6E, expression plasmid pTT28 [138] and as the source of *NT5E* gene, plasmid pCMV-N-Flag-NT5E (SinoBiological) was used. The final plasmid was designed to introduce sequence for His-tag instead of GPI signal sequence using VectorNTI software. Schemes of both plasmids (pTT28 and pCMV-N-Flag-NT5E) are depicted (see Figure 9 on page 30).

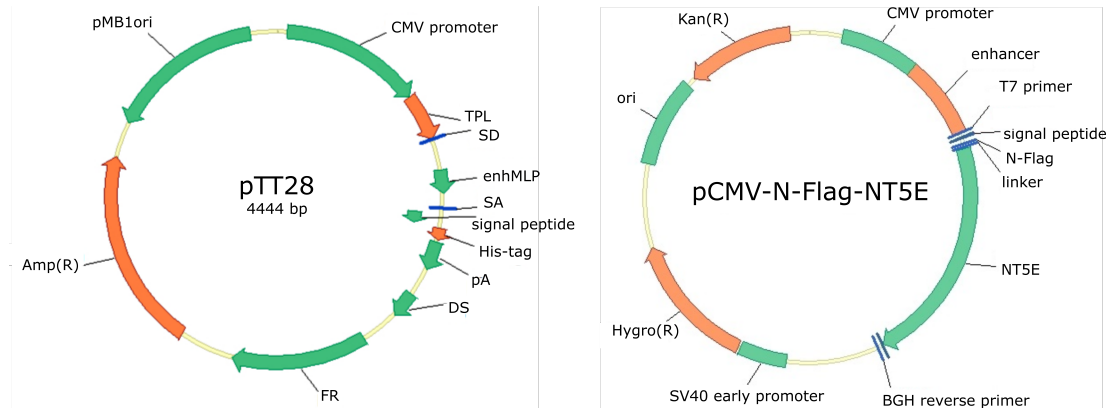


Figure 9: Plasmid maps used for cloning. On the left plasmid pTT28, on the right pCMV-N-Flag-NT5E.

5.2.2 Polymerase chain reaction

Polymerase chain reaction (PCR) was used for amplification of DNA sequence coding CD73. Reaction was performed in the total volume of 30 μ l, conditions are shown in the Table 1 on the page 31. Sequences of primers containing added cloning sites used for PCR are shown in Appendix on page 55. Products of PCR were separated by agarose electrophoresis (see section 5.2.3).

5.2.3 Agarose gel electrophoresis

TAE Buffer: 40mM Tris-HCl; 20mM CH_3COOH ; 1mM EDTA; pH 8.0

Sample Buffer: 40% (w/v) sucrose; 0.02% NaN_3 ; 0.1% (w/v) bromophenol blue

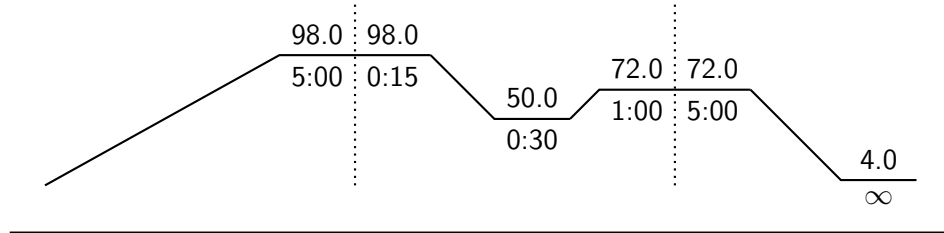
Whole sample from PCR was mixed with sample buffer (ratio 5:1) and analysed by horizontal agarose electrophoresis in 1% agarose prepared in TAE buffer with 10000x diluted fluorescent dye GelRed (Biotium). After 30 minutes at 120 V, DNA fragments of appropriate length were excised and isolated using QIAquick Gel Extraction Kit (Qiagen) according to the manufacturers instructions.

5.2.4 Cleavage using restriction endonucleases

Both expression plasmid and DNA fragment coding CD73 were cleaved using restriction endonucleases BamHI and NheI (New England Biolabs). Cleavage was performed in the total volume of 50 μ l for 60 minutes at 37°C. To 40 μ l

Table 1: Conditions of polymerase chain reaction.

	amount/ μl
pCMV-N-Flag-NT5E (1 ng/ μl)	1.0
R primer (100 μM)	0.3
F primer (100 μM)	0.3
dNTPs (10mM)	1.2
Phusion Buffer HF (5x)	6.0
Phusion polymerase (2 U/ μl)	0.3
MiliQ water	20.9



of DNA, 5 μl of 10x concentrated buffer and 0.5 μl of restriction endonuclease (20 U/ μl) was added. Overview of used nucleases and buffers is in Appendix on page 55. After cleavage, DNA fragments were analysed by agarose electrophoresis and extracted using QIAquick Gel Extraction Kit (see section 5.2.3 on page 30).

5.2.5 Ligation of DNA fragments

Plasmid and insert cleaved by corresponding endonucleases were ligated using T4 DNA ligase (New England Biolabs) for 60 minutes at 37 °C in the total volume 10 μl as depicted in the Table 2 on page 31. Control null ligation reaction without insert was performed in parallel.

Table 2: Reaction mixture of ligation reaction.

	amount/ μl
T4 DNA ligase Buffer (10x)	1
plasmid	1
insert or H ₂ O	5
T4 DNA ligase	1
water	2

5.2.6 Heat shock transformation of *E. coli*

Ligated plasmids were used for *E. coli* TOP10 transformation. Whole ligation reaction mixture was mixed with 30 μl of competent *E. coli* TOP10 cells and incubated 30 minutes on ice. After that, heat shock was performed in 42 °C for 90 sec followed by 1 minute cooling on ice. Subsequently, 300 μl of LB medium was added and the mixture was incubated for 1 hour at 37 °C without shaking. Preheated kanamycin (final concentration 100 $\mu\text{g}/\text{ml}$) agar plates were then treated with 200 μl of bacterial mixture and incubated at 37 °C overnight.

5.2.7 Minipreparation of plasmid DNA

The next day after *E. coli* transformation, 12.5 ml of LB media containing kanamycin (final concentration 100 µg/ml) was inoculated with single *E. coli* colony (performed in tetraplicate) and incubated at 37 °C overnight with shaking (220 RPM). The bacterial culture was then centrifuged (4000 g, 10 min) and DNA was isolated from the pellet using Zyppy Plasmid Miniprep Kit (Zymo Research) according to the manufacturers instructions. Concentration and purity of DNA was determined spectrophotometrically, using Nanodrop ND-1000 from 1 µl of the sample.

5.2.8 Maxipreparation of plasmid DNA

For large scale plasmid DNA preparation, the maxipreparation from 0.5 l media was performed. First, 0.5 l of antibiotics-containing LB media was inoculated with *E. coli* colony from agar plate and incubated at 37 °C overnight with shaking (220 RPM). Next day the cell culture was centrifuged (6000 g, 15 minutes) and plasmid DNA was isolated using Zyppy Plasmid Maxiprep Kit according to the manufacturers instructions. Concentration and purity of DNA was determined spectrophotometrically, using Nanodrop ND-1000 from 1 µl of the sample.

5.2.9 DNA sequencing

To make sure that cloning yielded correct products, the plasmids were sequenced. Sequencing mixture contained 450 ng of plasmid DNA and 2.5 µM primer in total volume of 10 µl. For sequencing, primers FWD-CD73-seq, FWD-pYD11-seq and REV-pTT28-seq were used. Primer sequences are listed in Appendix on page 55. Sequencing has been performed by GATC Biotech and data were analysed using program VectorNTI.

5.3 Protein expression in mammalian system HEK293–6E

For protein expression mammalian system HEK293–6E was used. All work with cell cultures was performed in sterile laminar flowbox. Suspension cell line HEK293–6E is designed for transient transfection so that it can be cultured in Erlenmeyer flask to higher densities. For transfection, it is recommended that cells have viability over 95% and density approximately $1,7 \cdot 10^6$ cells per millilitre. In order to achieve the right concentration, cells were diluted the day before to concentration $1 \cdot 10^6$ cells per millilitre in FreeStyle culture media and counted right before the transfection.

5.3.1 Small-scale transient transfection of HEK293–6E on a 6-well plate

Small-scale transient transfection was performed on a 6-well plate in 2 ml final volume. Experiment was performed in 4 wells – three wells were transfected with different DNA:PEI ratio, the fourth well was control well without transfection. Tested DNA:PEI ratios were 1:3, 1:5 and 1:7.

First 1.8 ml of cells were pipetted in to each well and then 200 µl of DNA mixture was added. In 1.5ml tube, 95 µl of transfection media OPTIMEM was mixed with 2 µg of plasmid DNA and then 14 µl (or 10 or 6 for other DNA:PEI ratios) of lPEI (linear polyethylenimine, 1 mg/ml) to the bottom of the tube and

gently mixed. After 10 minutes at RT whole mixture was added to cells. Plates with cells were then cultivated in rotating incubator (120 rpm) at 37 °C with 5% CO₂.

The production of the protein was monitored for five days starting on Day 3 after transfection. Sampling was done on daily bases, each day 100 µl of cells was centrifuged for 3 minutes on 250 g. Pellet was discarded and the supernatant was centrifuged once more for 10 minutes at 13000 g and stored in -20 °C before further analysis.

5.3.2 Large-scale transient transfection of HEK293–6E in Erlenmeyer flasks

Large-scale expression was performed in two 2L Erlenmeyer flasks, 500 ml of media in each with optimised DNA:PEI ratio 1:7. To 1 mg of plasmid DNA (prepared by maxipreparation) in 15 ml of OPTIMEM was added 7 ml of lPEI and subsequently the whole mixture was added to the cells. Cell density and viability was then monitored daily until Day 7, determined as optimal based on small-scale transfection.

5.3.3 Harvesting of secreted protein

Seven days after transient transfection of HEK293–6E, the expressed protein was harvested. Medium was first centrifuged for 10 minutes at 1500 g, cell pellet was discarded, and then supernatant was centrifuged for 35 minutes at 4000 g.

5.3.4 Affinity chromatography – purification using 6xHis-tag

From the cell-free medium His-tagged rhCD73 was purified using affinity chromatography. In the first round of purification, cOmplete His-Tag Purification Resin (Sigma-Aldrich) was used, followed by Ni-NTA Superflow (Qiagen) in the second. Both resins have the capacity for 40 mg of His-tagged protein per millilitre of the resin. Expected amount of protein was in the order of milligrams.

Buffer A: 300mM NaCl, 50mM Tris/HCl, pH 7.0

Buffer B: 300mM NaCl, 200mM imidazole, 50mM Tris/HCl, pH 7.0

First round of purification: 2 ml of resin suspension (50% of resin in buffer, column volume 1 ml) was applied on the 5ml chromatography column and equilibrated by ≈ 10 column volume (CV) of Buffer A. Equilibrated resin was then added to the supernatant of harvested protein in media. The adsorption of rhCD73 to the resin was performed overnight in 4 °C while shaking. Next day, all media was applied to the column and the flow-through was stored as FT1. The column was then washed by Buffer A (≈ 10 CV, W1) and Buffer A + 5mM imidazole² (≈ 5 CV, W2). The protein was eluted by Buffer A + 50mM imidazole (≈ 5 CV, E1) and then by Buffer B. Fraction of flow-through were sampled every five millilitres resulting in elution fraction E2 – E6. Purification process was subsequently monitored by 14% SDS PAGE.

²Buffer A with different concentration of imidazole was prepared by mixing of Buffer A and Buffer B.

Second round of purification: In the second round of purification, only slight modifications were made. Equilibrated resin NiNTA SuperFlow was added to the FT1 from the first round and adsorption of the protein was prolonged to two days. First washing step (W1) was performed with 50 CV of Buffer A, next steps were performed with increasing concentration of imidazole, resulting in another three washing steps and then six elution steps. Overview of amounts and imidazole concentration is in Table 3 on page 34.

Table 3: Overview of washing and elution fractions during first and second round of purification.

1 st round	W1	W2	E1	E2	E3	E4	E5	E6		
volume [ml]	10	5	5	5	5	5	5	5		
imidazole [mM]	0	5	50	200	200	200	200	200		
2 nd round	W1	W2	W3	W4	E1	E2	E3	E4	E5	E6
volume [ml]	50	50	10	10	10	10	10	10	10	10
imidazole [mM]	0	6.25	12.5	20	50	200	200	200	200	200

5.3.5 Protein concentration measurement

For measurement of protein concentration, Bradford Assay [139] with Coomassie Brilliant Blue G-250 was used. Bovine serum albumin (BSA) was used as standard.

5.4 SDS PAGE

Sample Buffer (6x): 350mM Tris/HCl (pH 6.8), 30% (v/v) glycerol, 2mM 2-mercaptoethanol, 350mM SDS, 180 μ M bromophenol blue

Running Buffer (5x): 140mM Tris/HCl (pH 8.8), 1.4M glycine, 20mM SDS

Stacking gel (6%): 250mM Tris/HCl (pH 6.8), 6.6% acrylamide³, 0.1% (w/v) SDS, 0.02% (v/v) TEMED⁴, 0.1% (w/v) APS

Separating gel (14%): 375mM Tris/HCl (pH 8.8), 14% acrylamide, 0.1% (w/v) SDS, 0.01% (v/v) TEMED, 0.1% (w/v) APS

Protein sample was mixed 5:1 with sample buffer and incubated 5 minutes at 96 °C for protein denaturation. After that, mixture was loaded on vertical SDS polyacrylamide gel and proteins were separated by electrophoresis for 60 minutes at 160 V. All blue marker (Bio-Rad) was used as protein standard.

Proteins on the gel were subsequently visualised by silver staining or specifically by western blot followed by immunodetection.

³Acrylamide and *N,N'*-Methylenebisacrylamide in the ratio 35.7:1.

⁴TEMED = Tetramethylethylenediamine, APS = ammonium persulfate, TEMED and APS are used for catalysis of polymerisation of acrylamide.

5.5 Silver staining of SDS polyacrylamide gel

Solution 1: 10% (v/v) acetic acid, 10% (v/v) methanol, 0.5% (v/v) formaldehyde

Solution 2: sodium thiosulfate pentahydrate (0.2 g/l), water solution

Solution 3: silver nitrate (2 g/l), 0.5% (v/v) formaldehyde

Solution 4: sodium carbonate (60 g/l), sodium thiosulfate (4 mg/l), 0.5% (v/v) formaldehyde

Solution 5: 12% (v/v) acetic acid, 50% (v/v) methanol

All steps were performed in RT on rotating shaker. Proteins on the gel were first fixed for 15 minutes in solution 1, then the gel was washed for 5 minutes in 50% (v/v) methanol. After 60 seconds exposure to the solution 2, the gel was quickly washed three times in distilled water and placed for 20 minutes to solution 3. The gel was washed three times in distilled water and proteins were finally visualised by solution 4. When bands were clearly visible, the gel was quickly washed by distilled water and placed for 10 minutes in the solution 5. Stained gel was then scanned on scanner.

5.6 Western blot and immunodetection

After electrophoresis, the gel and nitrocellulose membrane were washed in transfer buffer, surrounded by wet pieces of filtration paper and placed in the Mini Trans-Blot cell (Bio-Rad). Blotting was performed for 60 minutes at 100 V.

Transfer buffer: 192mM glycine, 25mM Tris/HCl, 10% (v/v) methanol

The membrane was subsequently blocked by 5 ml of Casein Blocker (1:20 in PBS) overnight in 4 °C. Next day, the membrane was washed in TBS and incubated 60 minutes in anti-polyHis iBody⁵ at RT. After three washes in TBS + 0.05% Tween 20 and one wash in TBS, His-tagged proteins were visualised using Odyssey CLx Infrared Imaging System (LI-COR) and data processed in ImageStudio software.

5.7 Malachite Green Assay for CD73 activity measurement

Enzymatic activity of rhCD73 was determined by detection of free phosphate cleaved from AMP using Malachite Green (MG) Phosphate Detection Kit (R&D Systems). All reactions were performed in 96-well clear plate in Assay Buffer.

Assay Buffer: 25 mM Tris/HCl, 5 mM MgCl₂, pH 7.5

Calibration curve: Phosphate standard (1M, provided by R&D Systems) was diluted 100x in Assay Buffer to 10 mM stock. To the standard calibration curve, the stock was diluted once more to have 100μM and additional five one-half serial dilutions were performed. Into a plate, 25 μl was loaded, to achieve a range of 0.039 to 2.5 nM (PO₄)³⁻ per well of standard curve.

⁵Jana Beranova et al., manuscript in preparation.

Standard MG Assay: Recombinant human CD73 was diluted to approximately 0.1 µg/ml and 25 µl (or 20 µl for inhibitor testing) was loaded into a plate. For inhibitor testing, 5 µl of tested inhibitor was added in this step. Plate with loaded protein (with or without inhibitor), standard curve and blanks (only Assay Buffer) was placed in water bath equilibrated to 37 °C for 20 minutes. The reaction was started by adding of 25 µl of 100µM AMP. Plate was covered by plate seal and incubated at 37 °C for 20 minutes. Reaction was stopped by adding of 10 µl of the Malachite Green Reagent A to all wells and the plate was incubated for 10 minutes at room temperature. For complex formation, 10 µl of the Malachite Green Reagent B was added to all wells, mixed and incubated for 20 minutes at room temperature. Absorbance at 620 nm was measured on plate reader Tecan. The activity was calculated according to the Equation (1):

$$\text{activity} = \frac{[\text{PO}_4^{3-}]}{t}, \quad (1)$$

where $[\text{PO}_4^{3-}]$ is concentration of released phosphate, calculated from standard curve and t is time of reaction.

Determination of Michaelis constant of rhCD73: For K_M measurement of rhCD73 the Malachite Green Assay was slightly modified. First 25 µl of substrate (range from 1600µM to 6.25µM) was added into the wells, in water bath equilibrated to 37 °C and the reaction was started by adding of 25 µl of rhCD73 (0.1 µg/ml). Following steps were the same as in the standard MG Assay. Experiment was performed in duplicate and data were fitted in GraphPad software.

Determination of inhibitory constant Standard MG Assay was performed for determination of K_i value with addition of inhibitor to the enzyme before adding of the substrate. By data fitting, IC_{50} value (concentration of inhibitor that causes 50% decrease of enzyme activity) is obtained. For competitive enzyme inhibition, relation between K_i and IC_{50} is described by Cheng-Prusoff equation:

$$K_i = \frac{\text{IC}_{50}}{1 + \frac{[\text{S}]}{K_M}}, \quad (2)$$

where K_i is inhibition constant (specific for the inhibitor, condition independent), K_M is Michaelis constant of the enzyme and $[\text{S}]$ is concentration of the substrate. Equation (2) is valid for low enzyme concentration.

5.8 DNA-linked Inhibitor Antibody Assay – DIANA

All DIANA experiments used in this thesis had the same setup. Plate was first coated by NeutrAvidin, then anti-poly-His polymer decorated with biotin was attached (NeutrAvidin–biotin interaction), in next step His-tagged rhCD73 (NTA–His-tag interaction) and at the end, probe (inhibitor of rhCD73 linked to oligonucleotide) was added. For inhibitor testing, in the last step, tested inhibitor was added together with the probe. Amount of bound probe was measured by qPCR.

5.8.1 Preparation of oligonucleotide conjugate as probes for DIANA

For probes preparation, copper catalysed azide-alkyne click reaction was used. Two types of inhibitor-azide (PSI 397 and PSI 405) and two types of oligonucleotide-alkyne (monovalent and bivalent) were tested resulting in four different probes. Inhibitors with linker and azide group (see Figure 18 on page 45) were prepared at Institute of Organic Chemistry and Biochemistry by Petr Šimon and oligonucleotides with alkyne group were purchased from Generi Biotech. First oligonucleotide and inhibitor were mixed together (to final concentration 200 μ M and 1000 μ M) and the reaction was catalysed by mixture of BTTP ligand (synthesised by Milan Vrabel), sodium ascorbate and CuSO₄ in 100mM HEPES buffer (pH 7.0), final ratio of oligonucleotide:inhibitor:BTTP:ascorbate:CuSO₄ was 2:-10:7.7:15.4:15.4. Mixture was incubated for two hours at 30 °C and then unbound reagents were washed out in ten cycles of concentrating on Amicon centrifuge filter (MWCO 10kDa) in TBS (10000 g, RT). Final concentration was determined using NanoDrop and analysed by LC-MS by Radko Soucek, IOCB.

5.8.2 Standard DIANA testing method

Buffer TBS: 20 mM Tris-HCl, pH 7.5, 150 mM NaCl

Buffer TBST: 20 mM Tris-HCl, pH 7.5, 150 mM NaCl, 0.05% Tween20 (w/v)

Buffer TBST': 20 mM Tris-HCl, pH 7.5, 150 mM NaCl, 0.1% Tween20 (w/v)

Buffer TBST'rh: Buffer TBST' + 5 μ M MgCl₂

Buffer TBST'p: Buffer TBST' CD73 + 1000x diluted casein blocker (SDT)

All incubation steps were performed in volume of 5 μ l at RT for 60 minutes (unless otherwise stated) and all washing steps were performed using Blue Washer instrumentation (Blue Cat Bio).

On Day 1, 96-well plate (4titude) was coated with NeutrAvidin. Into each well, 5 μ l of NeutrAvidin solution in TBS (10 ng/ μ l) was added by multichannel pipette, plate was covered by plate seal and incubated at RT, without shaking. After 60 minutes of incubation, 100 μ l of 5x diluted casein blocker in TBS (SDT) was added into each well and plate was covered by plate seal. The blockage was performed overnight at RT without shaking.

On Day 2, the wells were three times washed by 200 μ l of TBST. In next step, 5 μ l of 100nM anti-poly-His iBody⁶ in TBST' was added for 60 minutes. Excess of iBody was washed out by 200 μ l of TBST (three times). Further, rhCD73 in buffer TBST'rh was added. Amount of the protein was optimised, for details see section 5.8.3. After three washing steps (200 μ l of TBST each), incubation with probe in buffer TBST'p was performed (for details see sections 5.8.1, 5.8.3 and 6.5). Amount of the probe have been optimised together with amount of the protein. Together with the probe, into some wells, inhibitor PSB12379 was added (10 μ M for total displacement of the probe). After 60 minutes of incubation, unbound probe was washed out six times (200 μ l of TBST each). In the last step, 5 μ l of qPCR mix was added into each well, tightly sealed by foil and real-time PCR was performed in LightCycler instrument (Roche) as described in [140].

⁶Jana Beranova et al., manuscript in preparation.

Data were analysed in Light cycler 480 II software thus obtaining values of C_q as the value of qPCR cycle in inflexion point of the curve.

5.8.3 Optimisation of conditions

Conditions for rhCD73 DIANA were optimised, in each optimising step, condition resulting in higher assay window was chosen. Assay window, counted as difference of C_q for wells with and without inhibitor, was maximised, all experiments were thus performed both with and without presence of inhibitor PSB12379 during probe binding. Conditions have been optimised in four steps – first, best probe was chosen, then Probe buffer, followed by 2D screen (optimising amount of both rhCD73 and probe) and finally Protein buffer.

Probe selection: In the first experiment, the probe giving maximal assay window has been selected. Probe concentration was 500pM and rhCD73 ranged from 150 pg to 50 ng. All controls of unspecific binding have been performed – sandwich with all components but missing a) NeutrAvidin, b) anti-polyHis iBody, c) rhCD73, d) probe.

Buffer for probe binding: Instead of Buffer TBST'p for probe binding, six different buffers were examined – a) TBST', b) TBS + 0.1% Pluronic⁷, c) TBS + 1000x casein blocker + 0.1% Tween20, d) TBS + 1000x casein blocker + 0.01% Tween20, e) TBS + 1000x casein blocker + 0.1% Pluronic, f) TBS + 1000x casein blocker + 0.01% Pluronic. Amount of rhCD73 was 5 ng per well, probe concentration was 650pM.

Probe and rhCD73 amount optimisation: So called 2D screen was performed for optimal amount of rhCD73 and probe determination. Four concentration of probe and four concentration of rhCD73 have been investigated. For rhCD73: a) 1250 pg/well, b) 250 pg/well, c) 5000 pg/well and d) 10000 pg/well and for probe: a) 72pM, b) 217pM, c) 650pM and d) 1950pM.

Buffer for rhCD73 binding: Requirement for divalent ions in CD73 binding buffer have been investigated. Tested ions were Mg^{2+} , Zn^{2+} , Ca^{2+} , Co^{2+} and Ni^{2+} , all in two concentration – 5mM and 5μM. Also buffer without ions have been tested. For rhCD73 binding, ions were diluted in TBST', and subsequently for probes binding, also 1000x diluted casein was added. Amount of rhCD73 was 5 ng/well and probe concentration 2nM.

5.8.4 Determination of dissociation constant of probes

For K_d determination of probes, standard DIANA was performed with 5 ng of rhCD73 per well titrated with dilution series of the probe. The concentration of probe ranged from 10nM to 10pM. Values of dissociation constant were obtained by fitting of measured data by function (3):

$$[EP] = \frac{E_{tot} \cdot c_{pr}}{K_d + c_{pr}}, \quad (3)$$

where $[EP]$ is concentration of bound probe, E_{tot} is total amount of captured enzyme, c_{pr} is analytical concentration of the probe used for incubation and K_d is dissociation constant as described in [140].

⁷Pluronic is trade name for poloxamer, nonionic copolymer of polyoxypropylene and polyoxyethylene.

5.9 Enzyme-Linked Immunosorbent Assay – ELISA

For characterisation of specific interaction of anti-CD73 iBody with rhCD73, sandwich immunosorbent assay ELISA was used. All incubations were performed in 100 µl/well and washing steps in 200 µl/well.

Black 96-well Maxisorb plate (Nunc) was directly coated with 500ng/well of rhCD73 in TBS (60 minutes, RT, shaking) and then overnight blocked by 1% BSA in TBS at 4 °C while shaking. Next day, plate was four times washed by TBS + 0.1% Tween 20 for five minutes and then treated with dilution series of anti-CD73 iBody (range from 100nM to 100pM) and incubated for 60 minutes at RT. After five washing steps (TBS + 0.1% Tween 20, 5 min each), NeutrAvidin conjugated with horseradish peroxidase (HRP) in TBS + 0.1% Tween 20 was added (10ng/well). After one hour, wells were five times washed and 200 µl/well of chemiluminescence substrate was added and luminescence was immediately measured on spectrophotometric plate reader Tecan Infinite M1000 PRO. Experiment was performed in duplicate and as controls, wells without rhCD73 were used and wells without iBody. Data were obtained in duplicates and fitted in GraphPad 8.0.1. using total and non-specific binding as depicted in Figure 21 on page 48. Specific binding is described by equation (4):

$$y = \frac{B_{\max} \cdot x}{K_d + x}, \quad (4)$$

where B_{\max} is maximum signal in saturation and K_d is equilibrium binding constant, concentration of ligand needed for half-maximum binding at equilibrium.

Chemiluminescence substrate: 100 mM Tris/HCl, pH 8.8, 2.5 mM luminol, 2 mM 4-iodophenol, 0.02% H_2O_2

5.10 Preparation of stable transfectants expressing CD73

Adherent cell line HEK293 (approximately 50% confluency) was treated with transfection mixture of DNA and PEI in the ratio 1:3. To 2 µg of plasmid pCMV-N-Flag-NT5E (SinoBiological) in 100 µl of OPTIMEM medium, 6 µl of PEI (1 mg/ml) was added, gently mixed and let sit for 15 minutes at RT. After that, whole mixture was added dropwise to the cells. Cells were cultivated in IMDM media, after one week, treatment with antibiotic Hygromycin B (150 µg/ml) started and CD73 expressing clones have been selected. For proof of CD73 expression, flow cytometry was used.

5.11 Flow cytometry

Flow cytometry was used for the characterisation of the interaction of anti-CD73 iBody with CD73 expressing cell transfectants.

The adherent cell lines HEK293–T without CD73 and stable clone HEK293_–CD73 grown on 100mm Petri dishes in 10 ml of free IMDM media or IMDM + Hygromycin B (150 µg/ml) respectively, were used.

The medium was removed and cells were washed with PBS. Cells were then treated with trypsin/EDTA (0.25% (w/V) trypsin a 0.01% (w/V) EDTA)) for detaching of the cells from the dish and trypsinization was stopped by adding of fresh media. Cells were then centrifuged (250 g, 3 min), washed by PBS twice (1ml of PBS, centrifuge 250 g, 3 min) and placed in 1000 µl of media.

Amount of cells was counted using automated cell counter Countess (Thermo Fisher), the cells were diluted to $1.1 \cdot 10^6$ /ml concentration and cell suspension was poured into polypropylene 96-well plate with round bottom (90 μ l/well), so that every well contains $1 \cdot 10^5$ of cells. Dilution series of anti-CD73 iBody was added (range from 5 μ M to 64 pM in final) and as control of CD73 expression, 5 μ l of monoclonal anti-CD73 antibody labelled with phycoerythrin was used. The cells were incubated 60 minutes at 37 °C and then unbound iBody was washed out. Cells were first centrifuged (500 g, 5 min), twice washed with 200 μ l of PBS, finally resuspended in 200 μ l of PBS and analysed using flow cytometer BD LSR Fortessa™ (Becton, Dickinson and Company). The data were processed using software BD FACSDiva™ and FlowJo 10. The cytometer was set to analyse live single cells using side scatter and forward scatter. The example of gating (live and single cells selection), analysed by FACSDiva software, is shown in Figure 10 on page 40.

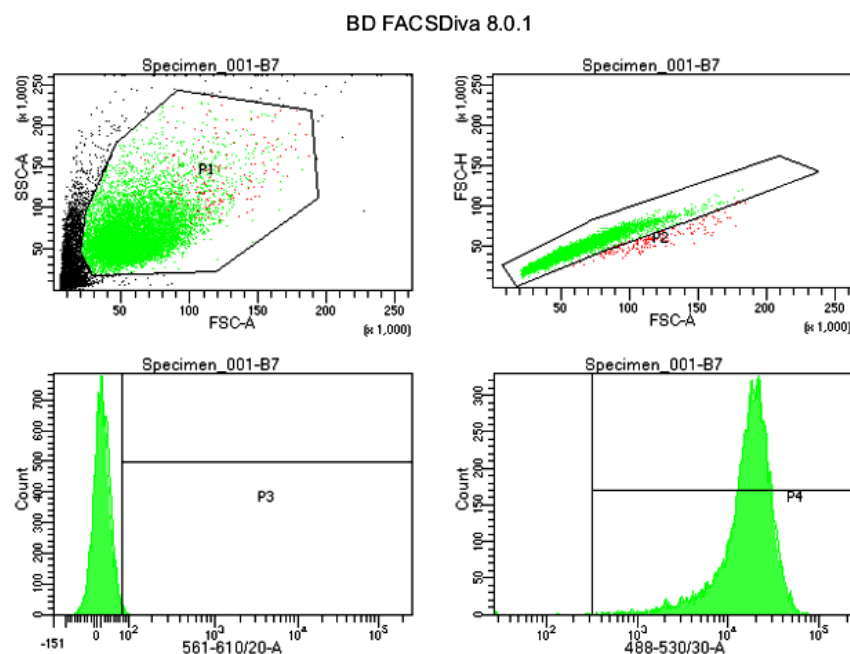


Figure 10: Example of gating in FACSDiva software. Population P1 are selected live cells, P2 only single cells. Population P3 and P4 are gated to be approximately 1% on negative cells, laser 561-610/20-A is for detection by monoclonal anti-CD73 antibody conjugated with phycoerythrin, laser 488-530/30-A is for detection of fluorescence of anti-CD73 iBody labelled with Atto488.

6 Results

6.1 Molecular cloning

Using PCR, *NT5E* coding gene (without GPI propeptide sequence) was amplified and cleavage sites for restriction endonucleases were inserted in the sequence. The reaction mixture was purified by agarose electrophoresis and the band around 2000 bp was isolated. After cleavage by restriction endonucleases, DNA was cleaned by agarose electrophoresis (see Figure 11 on page 41).

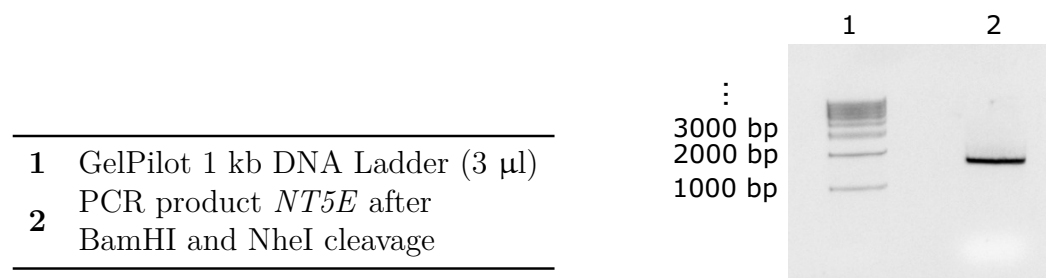


Figure 11: Agarose electrophoresis. 120 V, 30 min. The band of approximate 2000bp corresponds to cleaved DNA encoding *NT5E*.

Cleaved *NT5E* insert was then ligated into cleaved plasmid pTT28 and the whole mixture was used for *E. coli* transformation. Both ligated plasmid with insert (pTT28_CD73) and negative control without insert were seeded on agar plates treated with ampicillin. Twelve colonies grew on pTT28_CD73 plate and only one colony on the control plate, suggesting that ligation process was successful. Four of them were used for cultivation in LB media for plasmid miniprep. Concentration and purity of prepared DNA is in Table 4 on page 41. All inserts were incorporated properly, according to the sequencing, plasmid pTT28_CD73_2 was used for further experiments.

Table 4: Concentration and purity of prepared plasmids, measured on NanoDrop.

Sample	c [ng/ μ l]	abs 260/280	abs 260/230
pTT28_CD73_1	258	1.85	1.99
pTT28_CD73_2	372	1.87	2.25
pTT28_CD73_3	344	1.86	2.23
pTT28_CD73_4	367	1.87	2.25

6.2 Small-scale transfection

In previous experiments it was shown that optimal ratio of DNA and PEI for this cell line is 1:7 [141], for rhCD73 expression several transfection conditions were tested in small-scale experiments. Transfections have been done in 6-well plate and three DNA:PEI ratios were tested (1:3, 1:5 and 1:7). Media samples were taken for 5 days, starting on Day 3 after transfection. Amount of rhCD73 in media was determined by SDS electrophoresis followed by Western blotting with His-tag visualisation. As you can see in Figure 12 on page 42 and Figure 13

on page 42, the highest amount of rhCD73 was in media taken from Day 7 with DNA:PEI ratio 1:7.

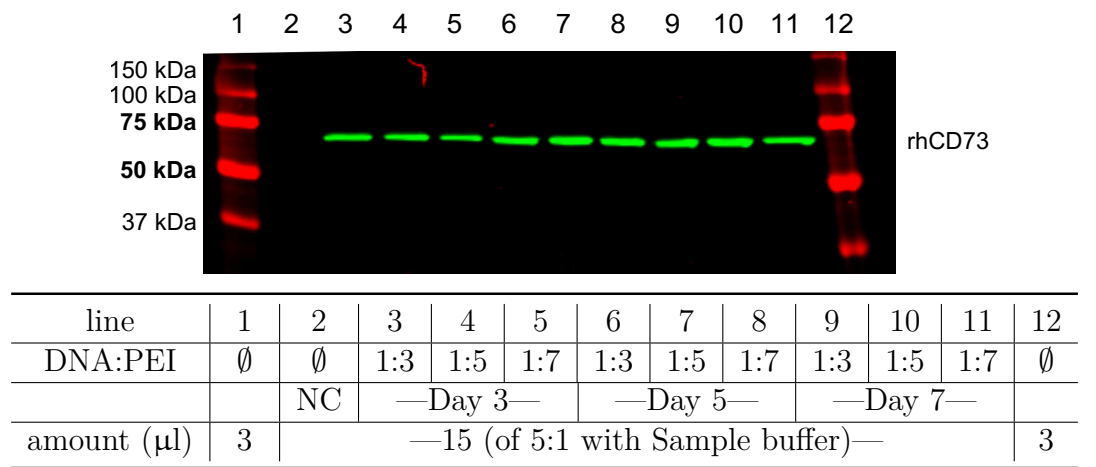


Figure 12: Small-scale transfection of HEK293–6E. Monitoring of rhCD73 production in mammalian system. The lines 1 and 12 contain All blue marker as protein standard. 14% SDS PAGE, 160V/60 min, Western blot, visualisation using α-poly His iBody 800 CW.

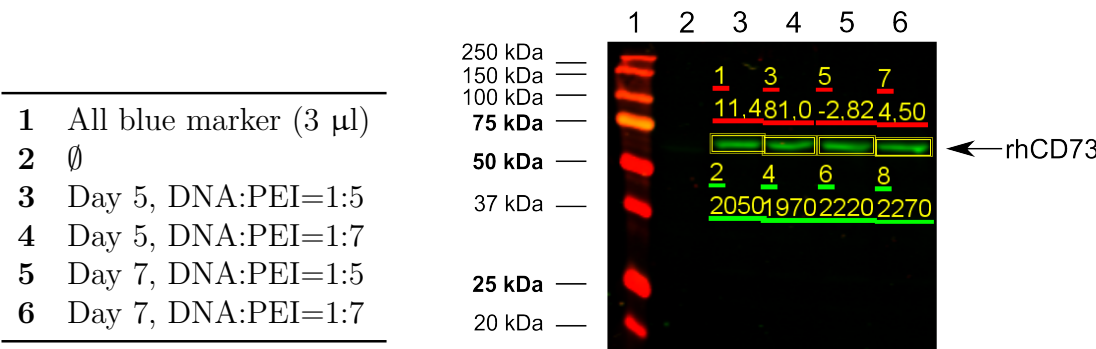


Figure 13: Small-scale transfection of HEK293–6E. Monitoring of rhCD73 production in mammalian system. The line 1 contains All blue marker as protein standard. The highest amount of rhCD73 according to ImageStudio software is in line 6. 14% SDS PAGE, 160V/60 min, Western blot, visualisation using α-poly His iBody 800 CW.

6.3 Large-scale expression and purification of rhCD73

Large-scale expression of rhCD73 was successfully performed in Erlenmeyer flasks and the protein was purified from medium in two rounds of purification using His-tag affinity chromatography. All purification steps were monitored by SDS electrophoresis and western blotting (see Figure 14 on page 43 and Figure 15 on page 43) and the activity of purified rhCD73 was tested using Malachite Green Assay.

All fractions containing rhCD73 were concentrated resulting in four fractions each with different purity and concentration. Elution steps 1 and 3 (E1, E3) from the first round of purification were concentrated together resulting in sample rhCD73 I-A, elution steps 4 to 7 resulted in sample rhCD73 I-B.

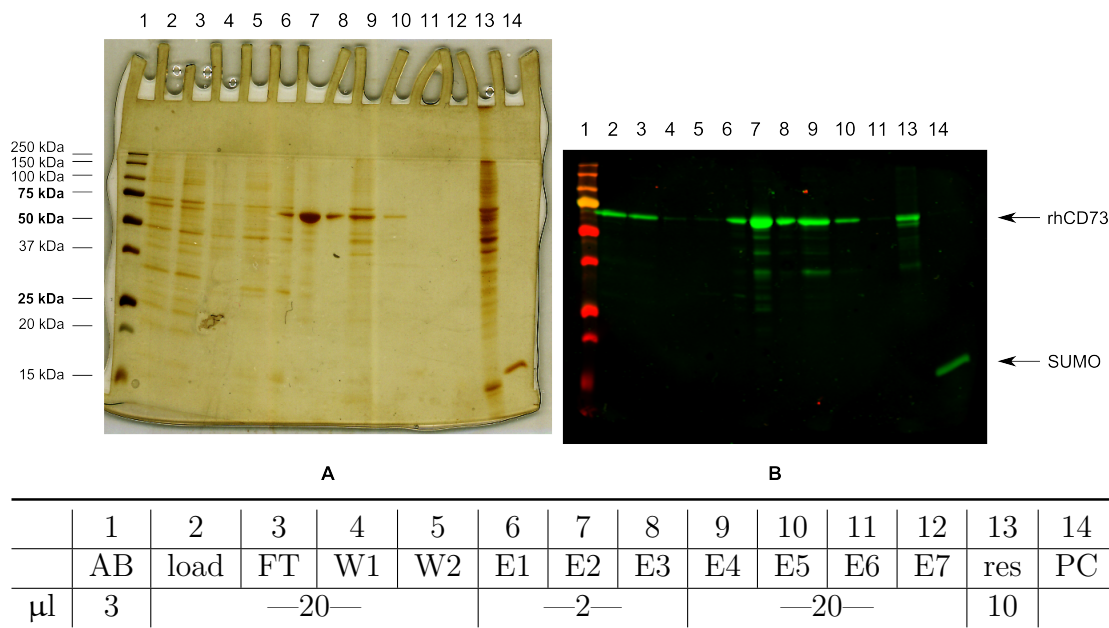


Figure 14: Monitoring of the first round of purification, 14% SDS PAGE, 160 V, 60 min; **A)** Ag staining, **B)** Western blot, visualisation using α -poly His iBody 800 CW; AB=All blue marker, FT=flow through, W=wash step, E=elution step, res= resin, PC= positive control, 6xHis SUMO, 200 ng.

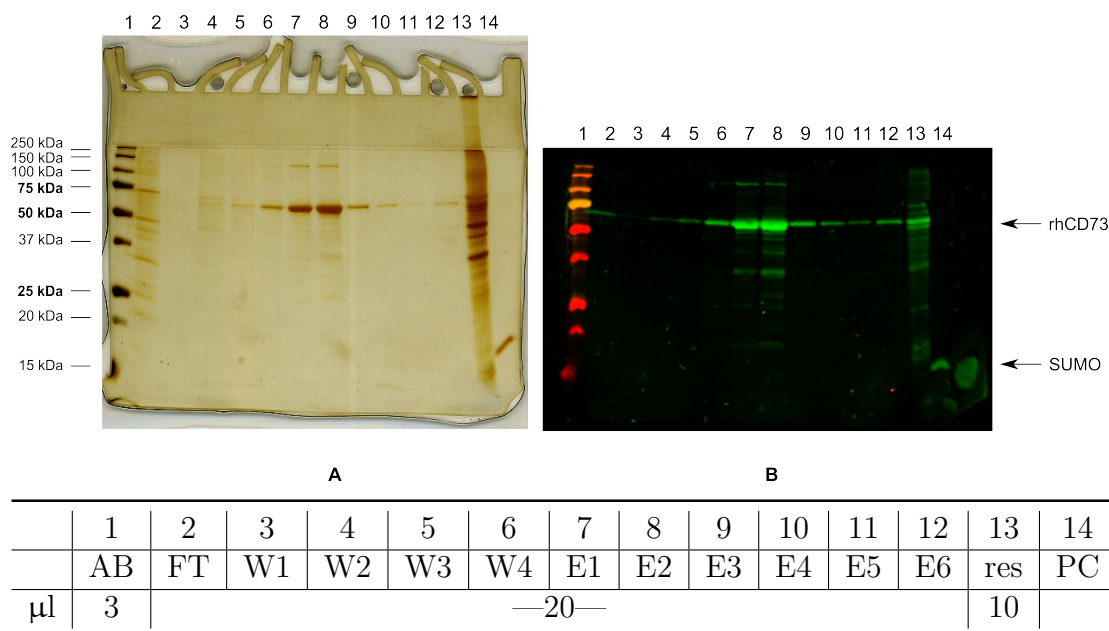


Figure 15: Monitoring of the second round of purification, 14% SDS PAGE, 160 V, 60 min; **A)** Ag staining, **B)** Western blot, visualisation using α -poly His iBody 800 CW; AB=All blue marker, FT=flow through, W=wash step, E=elution step, res= resin, PC= positive control, 6xHis SUMO, 200 ng.

Samples rhCD73 II are made of second round of purification, rhCD73 II-A of W4, E1, E2 and E3, sample rhCD73 II-B elution steps 4 to 9. Overview of concentration and amount of rhCD73 in different fractions is summarised in Table 5 on page 44. The total yield of rhCD73 is 3 mg per litre of media.

Table 5: Amount of CD73 in different fractions.

Sample	c [mg/ml]	amount [μg]
E2	0,27	1080
I-A	5,16	1342
I-B	0,80	120
II-A	1,24	372
II-B	0,21	42

Michaelis constant K_M of prepared rhCD73 was determined to be $24 \pm 3.7 \mu\text{M}$ and $V_{\text{max}} = 1.9 \pm 0.1 \mu\text{M (PO}_4\text{)}^{3-}/\text{min}$ using Malachite Green Assay. Data fitted in GraphPad 8.0.1. are in Figure 16 on page 44.

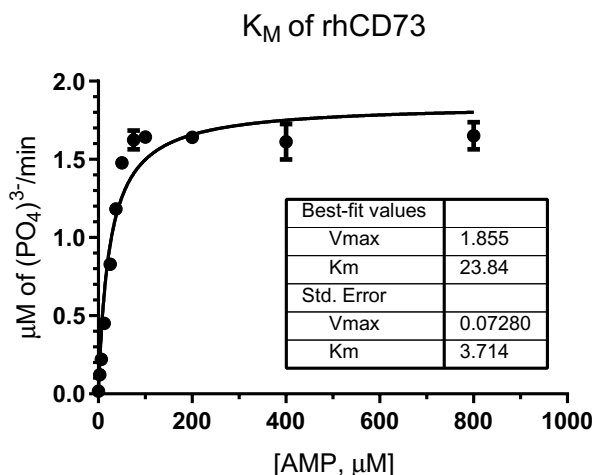


Figure 16: Determination of K_M of rhCD73 by Malachite Green Assay. Data were obtained from duplicates and fitted in GraphPad 8.0.1.

6.4 Inhibition constant measurement

For evaluation of K_i (inhibition constant) of the best published CD73 inhibitor PSB12379, Malachite Green Assay was used as described in 5.7. Obtained data (see Figure 17 on page 45) were fitted in GraphPad software, the IC_{50} value was calculated to be $\text{IC}_{50}(\text{PSB12379}) = 353 \pm 54 \text{ nM}$. For $[\text{S}] = 50 \mu\text{M}$ and $K_M = 24 \pm 3.7 \mu\text{M}$, according to the Equation (2) the $K_i = 114 \pm 4 \text{ nM}$.

Scaffold of the PSB12379 inhibitor was used to design probes for DIANA experiments and also for total displacement of probes in DIANA. Structures of two inhibitors⁸ used for copper catalysed azide-alkyne click reaction to oligonucleotides are depicted in Figure 18 on page 45.

⁸The synthesis of inhibitors was done by Petr Šimon at the Institute of Organic Chemistry and Biochemistry.

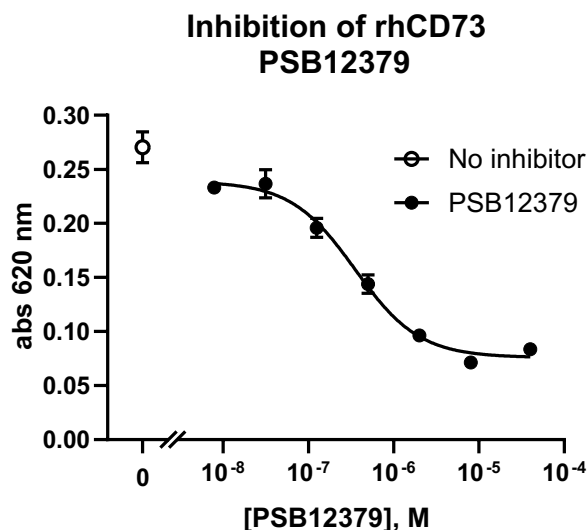


Figure 17: Inhibition of rhCD73 by PSB12379 measured by Malachite Green Assay and fitted in GraphPad 8.0.1. $IC_{50}(\text{PSB12379}) = 353 \pm 54 \text{ nM}$.

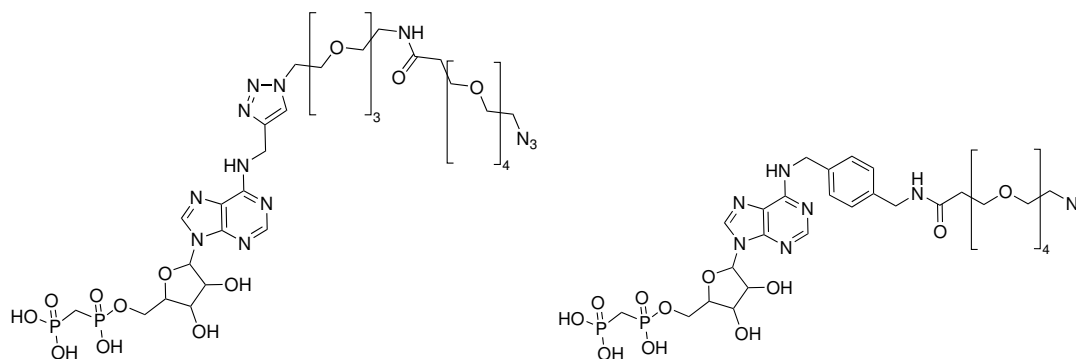


Figure 18: Structure of inhibitors PSI397 and PSI405 used for attachment to the oligonucleotide probes used in DIANA experiments.

6.5 DIANA

6.5.1 Probes preparation

Four probes were prepared for DIANA – probes P1 and P2 with PSI405 inhibitor and P3 and P4 with PSI397 inhibitor. Inhibition constants of those inhibitors and probes prepared were determined by Malachite Green Assay. Values of IC_{50} were in low micromolar range, probes approximately twice to ten times better than the original corresponding inhibitor. Inhibition of rhCD73 by PSI397 and the best probe P4 is depicted in Figure 19 on page 46.

6.5.2 Optimising of DIANA method for rhCD73

Conditions of DIANA method for rhCD73 inhibitor HTS screening of IOCB library were optimised giving the assay window $\Delta C_q = 8.7$. Best probe is probe P4 composed of PSI397 inhibitor and bivalent oligonucleotide. Best probe buffer is of a composition: TBS + 1000x casein blocker (SDT) + 0.1% Tween20. From 2D screen experiments, highest assay window is obtained using 1950pM probe and 5 ng of rhCD73 per well and regarding the rhCD73 binding buffer composi-

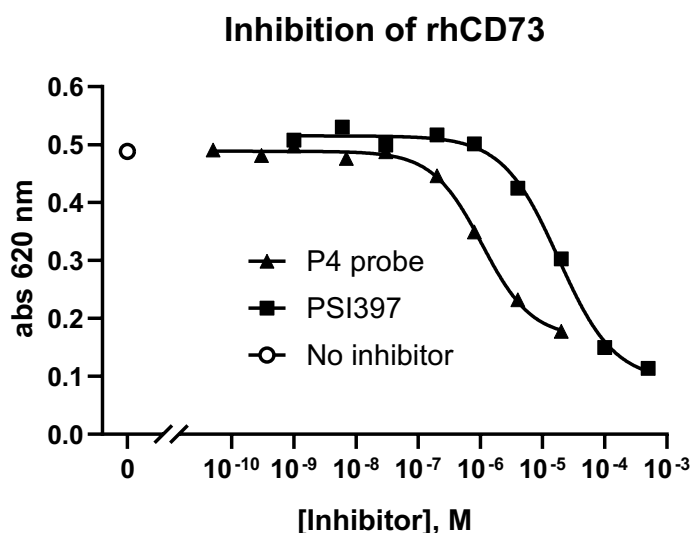


Figure 19: Inhibition of rhCD73 by PSI397 and P4 probe measured by Malachite Green Assay and fitted in GraphPad 8.0.1.
 $IC_{50}(\text{PSI397}) = 18.0 \pm 1.2 \mu\text{M}$, $IC_{50}(\text{P4 probe}) = 1.03 \pm 1.2 \mu\text{M}$.

tion, best results are with $5\mu\text{M Mg}^{2+}$. Results of optimisations are summarised in Table 6 on page 46.

Table 6: Overview of DIANA optimisation. In each optimising step, condition with larger assay window was chosen (highlighted in bold).

Probe selection					
P1	P2	P3	P4		
↓					
Probe buffer					
TBST'	TBS 0.1% Plur	TBS 1000x CB 0.1% Tw	TBS 1000x CB 0.01% Tw	TBS 1000x CB 0.1% Plur	TBS 1000x CB 0.01% Plur
↓					
2D screen/protein and probe amount					
rhCD73 \ Probe P4	72pM	217pM	650pM	1950pM	
1250 pg/well					
250 pg/well					
5000 pg/well				✓	
10000 pg/well					
↓					
Protein buffer – ions					
5μM	Mg ²⁺	Zn ²⁺	Ca ²⁺	Co ²⁺	Ni ²⁺
5mM	Mg ²⁺	Zn ²⁺	Ca ²⁺	Co ²⁺	Ni ²⁺

6.5.3 Determination of the dissociation constant of DIANA probe P4

For K_d determination of probes, 5 ng of rhCD73 per well was titrated with dilution series of probe P4. For fitting of obtained data, equation (3) was used, resulting in $K_d(\text{P4}) = 876$ pM.

6.5.4 High-throughput screening of IOCB library

For HTS of IOCB library, probe P4 was used. IOCB Compound Library is internal library collected from research groups at IOCB. It contains nucleosides, nucleotides and its analogues prepared by experienced medicinal chemists. Compounds are pooled into two 384-well plates, 11 compounds in each well.

Inhibitor screening of these two 384-well plates have been performed resulting in few positive wells. Testing of compounds present in these positive wells was performed resulting in several subnanomolar hits. Further evaluation of these compounds is in the progress.

6.6 Preparation and characterisation of anti-CD73 iBody

6.6.1 Anti-CD73 iBody preparation

Inhibitor with short linker (PSI389) for iBody preparation was synthesised by Petr Šimon at IOCB, the structure of PSI389 is depicted in Figure 20 on page 47. At Institute of Macromolecular Chemistry⁹, PSI389, biotin and fluorescence tag Atto488 was attached to the HPMA (*N*-(2-Hydroxypropyl) methacrylamide) copolymer [137]. The resulting anti-CD73 iBody has relative molecular weight 88 kDa and one molecule contains approximately 10 units of PSI389, 6 units of Atto488 and 17 units of biotin.

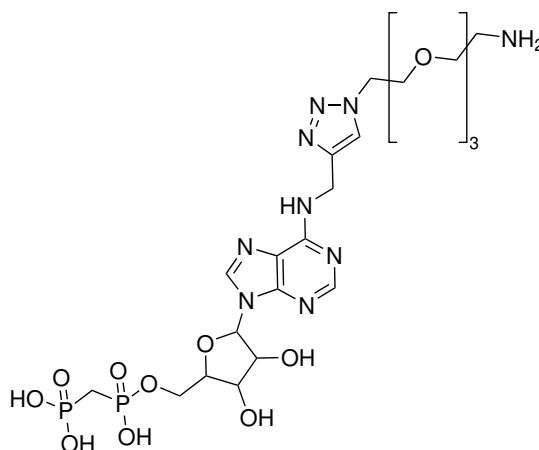


Figure 20: Structure of PSI389, inhibitor attached to HPMA polymer.

6.6.2 Characterisation of interaction between anti-CD73 iBody and rhCD73 using ELISA

Specific interaction of α -CD73 iBody with rhCD73 was characterised using ELISA (see Figure 21 on page 48). Constants for interaction of α -CD73 iBody and blocked rhCD73 are $B_{\max} = 2317881 \pm 152720$ RLU and $K_d = 9.1 \cdot 10^{-9} \pm 6.2 \cdot 10^{-9}$ M.

⁹Done by Dr. Vladimír Šubr and Dr. Libor Kostka.

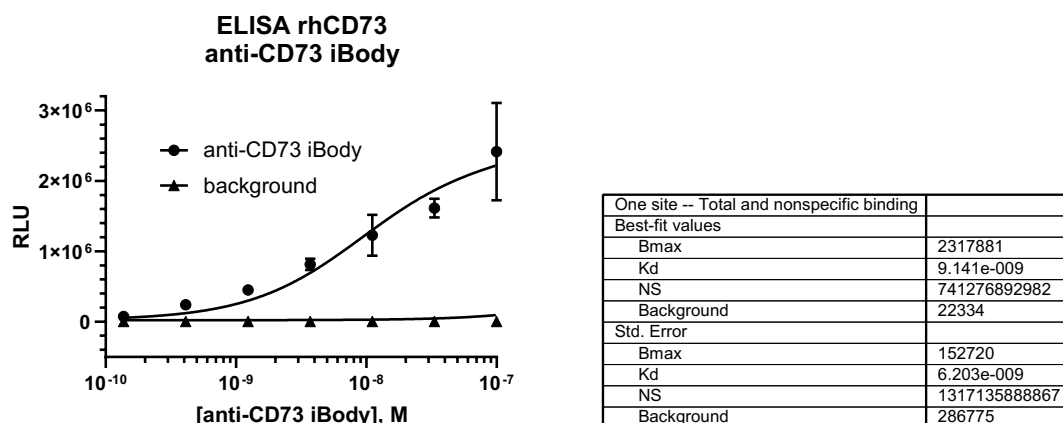


Figure 21: Polymer binding curve on rhCD73 in ELISA. Total interaction of anti-CD73 iBody with rhCD73 (anti-CD73 iBody) and non-specific binding (background) without rhCD73 with fitted curves. Data were obtained in duplicates. For data fitting GraphPad 8.0.1. software was used. One site: Total and non-specific binding. RLU= relative luminescence unit.

6.6.3 Flow cytometry measurement of binding of anti-CD73 iBody to cells

Characterisation of anti-CD73 iBody binding to CD73-expressing cells was performed on cell sorter FACS Fortessa. The specific binding of anti-CD73 iBody to CD73 expressing cells is depicted in Figure 22 on page 49 and binding curves of anti-CD73 iBody for both CD73 expressing and non-expressing cells are depicted in Figure 23 on page 49. The EC_{50} value of anti-CD73 iBody binding was determined to be approximately 100nM.

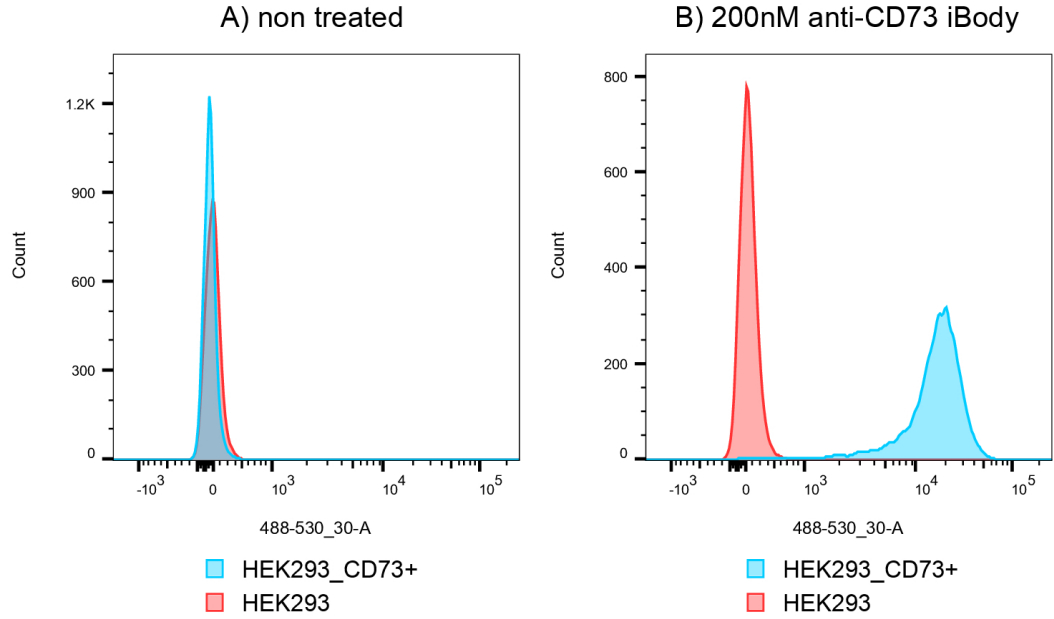


Figure 22: Specific polymer binding on CD73⁺ cells. Histograms of anti-CD73 iBody fluorescence (Atto488) of cells measured on FACS Fortessa. Data processed in FlowJo 10 software. **A)** Cells without staining **B)** Cells stained with 200nM anti-CD73 iBody.

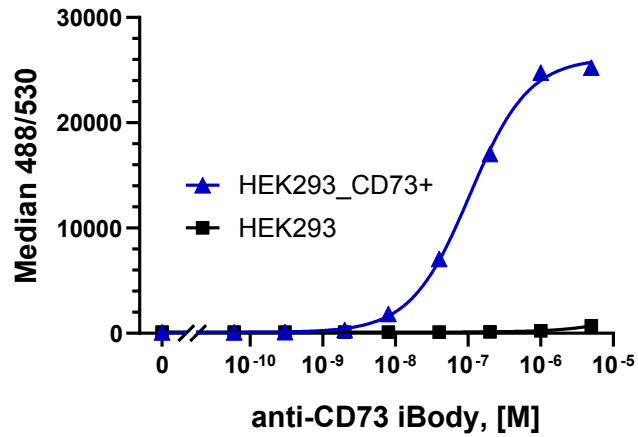


Figure 23: Binding curve of anti-CD73 iBody on cells. iBody binds specifically on CD73-expressing cell-transfectants with $EC_{50} \approx 100$ nM. Fluorescence of anti-CD73 iBody (Atto488) was measured on FACS Fortessa. Negative control cell line HEK293-T is not stained by the iBody, while CD73-expressing cells are well-stained.

7 Discussion

Cancer is one of the most common causes of death, every year millions of people die worldwide. New strategies to cancer treatment are intensively studied and in the last decades, immunotherapy with involvement of patient's own immune system shows first successes. However, many highly potent approaches do not show desired efficacy and often have only minimal or no effect at all. Many therapies fail because of the immunosuppressive tumour microenvironment.

The involvement of purinergic signalling pathway has been proven to contribute to the immunosuppressive tumour microenvironment with key ectonucleotidase CD73.

In this master thesis, first, I have designed a plasmid for expression in mammalian system HEK293–6E coding recombinant human CD73 without signal sequence for GPI anchor but containing sequence for His-tag. The mammalian expression system was chosen because of the presence of *N*-glycosylation on mature protein that can not be done in neither bacterial nor insect S2 expression system. The evidence of expression of CD73 without GPI anchor retaining enzymatic activity was found in publications and the attachment of His-tag to the *C*-terminus should also have no effect on activity, according to the literature.

Plasmid pTT28, suitable for transient transfection of HEK293–6E cells, was used as the donor plasmid. As the source of *NT5E* gene, the plasmid pCMV-N-Flag-NT5E was chosen. The same plasmid was further used for preparation of stable clones expressing whole-length CD73. The proclaimed *N*-Flag tag will not be present on the mature protein because the *N*-Flag sequence will be cleaved off together with the signal peptide.

The expression plasmid was prepared by classic molecular cloning techniques including PCR of *NT5E* from the source plasmid, cleavage of both plasmids (restriction endonucleases BamHI and NheI) followed by T4 ligation. The PCR process and cleavage was controlled by horizontal agarose electrophoresis, the ligation and *E. coli* transformation efficiency by comparison of ampicillin-containing agar plates inoculated by *E. coli* transformed by ligation mixture containing vector with insert and null ligation without insert. The ratio of numbers of colonies on plates was 12:1, suggesting that the ligation process was successful. From the pTT28_CD73 plate, four colonies were used for further DNA isolation. All four plasmids were sequenced using three different primers – one reverse and one forward on the edges of cleavage sites and one forward, CD73 specific – and DNA sequences corresponded with expectations. For expression, plasmid pTT28_CD73_2 was used for the highest purity according to NanoDrop measurement.

The cost of expression in mammalian system is high, so the transfection conditions and length of expression have been optimised in small-scale to gain maximal amount of the protein. The pTT28 plasmid is suitable for transient transfection of HEK293–6E by complexes of DNA with cationic polymer polyethylenimine (PEI). Three DNA:PEI ratios have been tested – 1:3, 1:5 and 1:7. After transfection, samples of media have been taken every day, starting on Day 3, and stored at -20 °C before further analysis. Amount of the protein in media was determined by SDS-PAGE followed by Western blot with anti-polyHis iBody visualisation. There were no considerable differences, yet the best conditions according to the Western blot were transfection by DNA mixed with PEI in the ratio 1:7 and seven

days of expression. These findings correspond with those previously observed in our laboratory [141].

Expression of rhCD73 in large-scale was done in total volume of 1000 ml with optimised transfection conditions and harvested after seven days. Protein was purified via His-tag affinity chromatography and the purification process was monitored by SDS-PAGE followed by silver staining of the gel and by Western blot with anti-polyHis iBody visualisation. Due to the significant amount of rhCD73 in the flow-through fraction, second round purification was still necessary. The elution fractions from the first round contained notable amount of impurities, in the second round, more washing steps were included with increased wash volumes. After second round, amount of rhCD73 in the flow-through fraction was negligible and purity of elution fractions was sufficient, with no need of further purification. The protein yield was about 3 mg of purified rhCD73 per one litre of expression media.

For activity measurement of rhCD73, Malachite Green Assay was established. Michaelis constant of rhCD73 K_M of $23.84 \pm 3.71 \mu\text{M}$ was determined using this method, which corresponds with literature. After that, inhibition constant of PSB12379 was determined using Malachite Green as $K_i = 113.8 \pm 3.74 \text{ nM}$, which is about two orders of magnitude higher than published [78]. The data were measured repeatedly with the same result. One explanation for discrepancy of measured data could be different methods used for K_i determination. Later, K_i of PSB12379 was determined using DIANA with K_i in low nanomolar range, consistent with the original publication, thus implying a possible technical error of used Malachite Green Assay.

For high-throughput screening of IOCB library was chosen immuno-qPCR-based DIANA method with low consumption of protein and chemicals. For probe preparation necessary for DIANA method, Petr Šimon synthesised two inhibitors (PSI397 and PSI405) with scaffold derived from PSB12379. Both of them were attached to two kinds of oligonucleotides by azide-alkyne click reaction resulting in four probes P1 to P4. Conditions of rhCD73 DIANA method were optimised in several steps, with focus on the maximisation of an assay window defined as a difference between signal of inhibited and non-inhibited protein.

At first, proof-of-concept experiment was done with all four probes at several conditions. The best probe seemed to be the probe P4 (triazole containing PSI397 and bivalent oligonucleotide). Furthermore, influence of probe binding buffer composition was studied, revealing maximal assay window in buffer of composition of TBS + 1000x casein blocker (SDT) + 0.1% Tween20 confirming expected importance of detergent. Subsequently, four rhCD73 concentrations and four probe concentration were tested to maximise signal to noise ratio. As optimal amount of reagents, 5 ng of rhCD73 and 2nM probe, were chosen in this assay taking into consideration low consumption of reagents, sufficient assay window and linear range of the assay. In the next step, influence of divalent ions in protein binding buffer was examined in two concentration of ions – 5 μM and 5 mM. Common, biologically relevant, divalent ions have been taken into consideration – Mg^{2+} , Zn^{2+} , Ca^{2+} , Co^{2+} and Ni^{2+} . In the obtained data, trend of lower concentration being better for all studied ions was observable. The highest assay

window was achieved by 5 μM Mg^{2+} , comparable to buffer with no divalent ions. The value of ΔC_q reached 8.7 value, which is more than sufficient for HTS and thus further optimisation was not performed.

To determine K_i of an inhibitor, the information of the probe K_d is essential. Titration of probe in DIANA experiment was done to determine K_d . The titration confirmed subnanomolar K_d value.

With great help of Katka Rojíková, HTS of IOCB library was performed with optimised DIANA. Preliminary results have been already obtained, evaluation of them is in progress at the time of writing this thesis. In the next steps, inhibition constants of found hits are going to be confirmed using orthogonal activity assay.

Probes with different inhibitors will be tested, since tested PSI397 and PSI405 differ in the length of the linker and in the core of the inhibitor (triazole versus benzyl). Thus, comparison of binding properties can not be currently drawn.

The other aim of my thesis was characterisation of anti-CD73 iBody interaction with recombinant CD73 and with cell lines expressing surface CD73. For iBody preparation, Petr Šimon synthesised another inhibitor PSI389, which was attached to the HPMA polymer at the Institute of Macromolecular Chemistry together with biotin and fluorescence tag Atto488 for visualisation. Basic analysis of prepared iBody done at Institute of Macromolecular Chemistry revealed that one molecule contains approximately ten units of PSI389, six units of Atto488 and seventeen units of biotin.

Inhibitory ability of anti-CD73 iBody was measured by Malachite Green and DIANA with low nanomolar K_i . Interaction of anti-CD73 iBody with immobilised rhCD73 was characterised using ELISA with direct adsorption of rhCD73 on the plate. To obtain K_d value of anti-CD73 iBody, 500 ng of rhCD73 per well was titrated with the dilution series of iBody. The obtained K_d value had a large error $K_d = 9.141 \cdot 10^{-9} \pm 6.203 \cdot 10^{-9}$ M, the data are therefore going to be remeasured. Inverse ELISA sandwich with immobilised iBody can not be used because of the high nonspecific binding of the protein.

Furthermore, cell lines stably expressing membrane-bound CD73 have been prepared by transfection with pCMV-N-Flag-NT5E plasmid. For stably expressing CD73 transfectants was chosen HEK293 cell line that does not have intrinsic expression of CD73. Effective transfection was showed by anti-CD73 antibody labelled by phycoerythrin followed by flow cytometry. According to the flow cytometry, the size and shape of the cell after transfection have not changed, but it was observed that CD73 expression affects cells adhesion ability.

Specific interaction of anti-CD73 iBody with CD73 was demonstrated using flow cytometry. HEK293 cells both expressing and non-expressing CD73 were incubated with dilution series of iBody. As it is shown in Figure 23 on page 49, the interaction of the iBody with cells is highly specific, first signs of unspecific binding are in 1000nM concentration. That is about 5000 times higher than K_i of iBody measured on rhCD73.

The interaction of anti-CD73 iBody with rhCD73 and with cell transfectants has been studied using few of possible biochemical methods so far. In the near future, other techniques will be used. To determine K_d , surface plasmon resonance (SPR) can be used, which is an orthogonal assay to ELISA. First SPR

experiments have been done, further optimisation of this method is necessary. The anti-CD73 iBody could be also used for pull-down (or immunoprecipitation) of rhCD73. Regarding interaction with cell transfectants, binding to the CD73⁺ cells will be measured by confocal microscopy as well as on peripheral blood mononuclear cells from human donors. The confocal microscopy can also show internalisation and trafficking of the CD73 labelled with iBody.

8 Conclusion

Recombinant human CD73 without GPI anchor was successfully prepared in mammalian expression system HEK293–6E and purified using His-tag affinity chromatography. The yield of the protein was 3 mg of rhCD73 per litre of media.

Stable clones of HEK293 cell line expressing CD73 have been prepared (HEK-293_CD73⁺) and the presence of CD73 on the surface was verified by antibody staining and flow cytometry measurement.

In the cooperation with Petr Šimon and Institute of Macromolecular Chemistry, anti-CD73 iBody has been prepared. This polymer conjugate contains inhibitor of CD73, biotin and fluorescence tag Atto488. Interaction of this polymer with rhCD73 have been studied and K_d of this interaction have been determined using ELISA.

Interaction of the anti-CD73 iBody with HEK293_CD73⁺ have been studied as well. The specific staining of CD73-positive cells was proved and EC_{50} of interaction was measured by titration of iBody on cells.

For detection of CD73, DIANA was adapted for the rhCD73. Conditions of DIANA setup have been optimised – namely buffers composition and amount of probe and protein – to gain appropriate assay window for high-throughput screening. Finally, high-throughput screening of compounds prepared at IOCB Prague – so called IOCB library – was performed using DIANA method and several subnanomolar hits were found.

In the near future, the hits found by HTS are going to be tested by orthogonal activity assay based on free phosphate determination to confirm the data.

In this thesis, I have successfully characterised antibody mimeticum of CD73 with low nanomolar binding properties and established HTS assay for inhibitor screening of CD73. These findings allow further investigation of highly biological relevant enzyme CD73 and modulate immunosuppressive tumour microenvironment.

Appendix

Primer sequences

Sequences of primers used for PCR (see page 30) and sequencing of prepared plasmids (see page 32).

Table 7: Sequences of primers used for PCR and sequencing.

	primer name	sequence (5' \rightarrow 3')
R primer	REV-CD73-BamHI	aaaggatccgaaaacttgatccgaccttc
F primer	FWD-CD73-NheI	aaagctagctgggagcttacgattttgcac
F primer sequencing	FWD-CD73-seq	ctttacacaggcaatccacct
F primer sequencing	FWD-pYD11-seq	gggtgagtactccctctca
R primer sequencing	REV-pTT28-seq	cagttggcaagttgtaccaac

Restriction endonucleases used for DNA cleavage

Cleavage sites of used restriction endonucleases and recommended buffers (see page 30).

Table 8: Condition of cleavage by restriction endonucleases.

enzyme	recommended buffer	cleavage site
BamHI	NEB 3.1	G[GATC C C CTAG]G
NheI	NEB 2.1	G[CTAGC C GATC]G

References

- [1] Lind, M. J. Principles of cytotoxic chemotherapy. *Medicine* **36**, 19–23. doi:10.1016/j.mpmed.2007.10.003 (Jan. 2008).
- [2] Chan, J. K. C., Ng, C. S. & Hui, P. K. A simple guide to the terminology and application of leucocyte monoclonal antibodies. *Histopathology* **12**, 461–480. doi:10.1111/j.1365-2559.1988.tb01967.x (May 1988).
- [3] EMBL-EBI. [Online]. *UniProt* <https://www.uniprot.org/>. [Cited on Apr. 10, 2019].
- [4] OpenStax. [Online]. *Anatomy & Physiology* version 8.25. <https://cnx.org/contents/FPtK1zmh@8.25:xEZkXdm8@5/Anatomy-of-the-Lymphatic-and-Immune-Systems>. [Cited on Apr. 2, 2019].
- [5] Chen, D. & Mellman, I. Oncology Meets Immunology: The Cancer-Immunity Cycle. *Immunity* **39**, 1–10. doi:10.1016/j.immuni.2013.07.012 (July 2013).
- [6] Mullard, A. New checkpoint inhibitors ride the immunotherapy tsunami. *Nat. Rev. Drug Discovery* **12**, 489–492. doi:10.1038/nrd4066 (July 2013).
- [7] Dunn, G. P., Bruce, A. T., Ikeda, H., Old, L. J. & Schreiber, R. D. Cancer immunoediting: from immunosurveillance to tumor escape. *Nat. Immunol.* **3**, 991–998. doi:10.1038/ni1102-991 (Nov. 2002).
- [8] Garland, S. M. *et al.* Quadrivalent Vaccine against Human Papillomavirus to Prevent Anogenital Diseases. *N. Engl. J. Med.* **356**, 1928–1943. doi:10.1056/nejmoa061760 (May 2007).
- [9] Lee, S. & Margolin, K. Tumor-Infiltrating Lymphocytes in Melanoma. *Curr. Oncol. Rep.* **14**, 468–474. doi:10.1007/s11912-012-0257-5 (Aug. 2012).
- [10] Tran, E. *et al.* T-Cell Transfer Therapy Targeting Mutant KRAS in Cancer. *N. Engl. J. Med.* **375**, 2255–2262. doi:10.1056/nejmoa1609279 (Dec. 2016).
- [11] Tran, E. *et al.* Cancer Immunotherapy Based on Mutation-Specific CD4+ T Cells in a Patient with Epithelial Cancer. *Science* **344**, 641–645. doi:10.1126/science.1251102 (May 2014).
- [12] Zacharakis, N. *et al.* Immune recognition of somatic mutations leading to complete durable regression in metastatic breast cancer. *Nat. Med.* **24**, 724–730. doi:10.1038/s41591-018-0040-8 (June 2018).
- [13] Grupp, S. A. *et al.* Chimeric Antigen Receptor–Modified T Cells for Acute Lymphoid Leukemia. *N. Engl. J. Med.* **368**, 1509–1518. doi:10.1056/nejmoa1215134 (Apr. 2013).
- [14] National Cancer Institute. [Online]. *FDA Approves Second CAR T-Cell Therapy for Lymphoma* <https://www.cancer.gov/news-events/cancer-currents-blog/2018/tisagenlecleucel-fda-lymphoma>. [Cited on Jan. 30, 2019].
- [15] Lee, D. W. *et al.* Current concepts in the diagnosis and management of cytokine release syndrome. *Blood* **124**, 188–195. doi:10.1182/blood-2014-05-552729 (May 2014).

- [16] Santomasso, B. D. *et al.* Clinical and Biological Correlates of Neurotoxicity Associated with CAR T-cell Therapy in Patients with B-cell Acute Lymphoblastic Leukemia. *Cancer Discov.* **8**, 958–971. doi:10.1158/2159-8290.cd-17-1319 (June 2018).
- [17] Ying, Z. *et al.* A safe and potent anti-CD19 CAR T cell therapy. *Nat. Med.* doi:10.1038/s41591-019-0421-7 (Apr. 2019).
- [18] Mølhøj, M. *et al.* CD19-/CD3-bispecific antibody of the BiTE class is far superior to tandem diabody with respect to redirected tumor cell lysis. *Mol. Immunol.* **44**, 1935–1943. doi:10.1016/j.molimm.2006.09.032 (Mar. 2007).
- [19] Nagorsen, D., Bargou, R., Rüttinger, D., Kufer, P., Baeuerle, P. A. & Zugmaier, G. Immunotherapy of lymphoma and leukemia with T-cell engaging BiTE antibody blinatumomab. *Leuk. Lymphoma* **50**, 886–891. doi:10.1080/10428190902943077 (Jan. 2009).
- [20] Breitbach, C. J., Lichty, B. D. & Bell, J. C. Oncolytic Viruses: Therapeutics With an Identity Crisis. *EBioMedicine* **9**, 31–36. doi:10.1016/j.ebiom.2016.06.046 (July 2016).
- [21] Zamarin, D. *et al.* Localized Oncolytic Virotherapy Overcomes Systemic Tumor Resistance to Immune Checkpoint Blockade Immunotherapy. *Sci. Transl. Med.* **6**, 226ra32–226ra32. doi:10.1126/scitranslmed.3008095 (Mar. 2014).
- [22] Bell, J. & McFadden, G. Viruses for Tumor Therapy. *Cell Host Microbe*. **15**, 260–265. doi:10.1016/j.chom.2014.01.002 (Mar. 2014).
- [23] Kaufman, H. L. & Bines, S. D. OPTIM trial: a Phase III trial of an oncolytic herpes virus encoding GM-CSF for unresectable stage III or IV melanoma. *Future Oncol.* **6**, 941–949. doi:10.2217/fon.10.66 (June 2010).
- [24] Lin, C., Xiang, G., Zhu, X., Xiu, L., Sun, J. & Zhang, X. Advances in the mechanisms of action of cancer-targeting oncolytic viruses (Review). *Oncology Lett.* doi:10.3892/ol.2018.7829 (Jan. 2018).
- [25] Leach, D. R., Krummel, M. F. & Allison, J. P. Enhancement of Antitumor Immunity by CTLA-4 Blockade. *Science* **271**, 1734–1736. doi:10.1126/science.271.5256.1734 (Mar. 1996).
- [26] Qureshi, O. S. *et al.* Trans-Endocytosis of CD80 and CD86: A Molecular Basis for the Cell-Extrinsic Function of CTLA-4. *Science* **332**, 600–603. doi:10.1126/science.1202947 (Apr. 2011).
- [27] Hodi, F. *et al.* Improved Survival with Ipilimumab in Patients with Metastatic Melanoma. *N. Engl. J. Med.* **363**, 1290–1290. doi:10.1056/nejmx100063 (Sept. 2010).
- [28] Okazaki, T. & Honjo, T. PD-1 and PD-1 ligands: from discovery to clinical application. *Int. Immunol.* **19**, 813–824. doi:10.1093/intimm/dxm057 (June 2007).

- [29] Brahmer, J. R. *et al.* Survival and long-term follow-up of the phase I trial of nivolumab (Anti-PD-1; BMS-936558; ONO-4538) in patients (pts) with previously treated advanced non-small cell lung cancer (NSCLC). *J. Clin. Oncol.* 8030–8030. doi:10.1200/jco.2013.31.15_suppl.8030 (May 2013).
- [30] Anderson, A., Joller, N. & Kuchroo, V. Lag-3, Tim-3, and TIGIT: Co-inhibitory Receptors with Specialized Functions in Immune Regulation. *Immunity* **44**, 989–1004. doi:10.1016/j.immuni.2016.05.001 (May 2016).
- [31] Marin-Acevedo, J. A., Dholaria, B., Soyano, A. E., Knutson, K. L., Chumsri, S. & Lou, Y. Next generation of immune checkpoint therapy in cancer: new developments and challenges. *J. Hematol. Oncol.* **11**. doi:10.1186/s13045-018-0582-8 (Mar. 2018).
- [32] Soularue, E. *et al.* Enterocolitis due to immune checkpoint inhibitors: a systematic review. *Gut* **67**, 2056–2067. doi:10.1136/gutjnl-2018-316948 (Aug. 2018).
- [33] Ledford, H. Promising cancer drugs may speed tumours in some patients. *Nature* **544**, 13–14. doi:10.1038/nature.2017.21755 (Mar. 2017).
- [34] Wong, D. J., Lee, J., Choo, S. P., Thng, C. H. & Henedige, T. Hyperprogressive disease in hepatocellular carcinoma with immune checkpoint inhibitor use: a case series. *Immunotherapy* **11**, 167–175. doi:10.2217/imt-2018-0126 (Feb. 2019).
- [35] Wang, M. *et al.* Role of tumor microenvironment in tumorigenesis. *J. Cancer*. doi:10.7150/jca.17648 (2017).
- [36] Belli, C. *et al.* Targeting the microenvironment in solid tumors. *Cancer Treat. Rev.* **65**, 22–32. doi:10.1016/j.ctrv.2018.02.004 (Apr. 2018).
- [37] Kalluri, R. & Zeisberg, M. Fibroblasts in cancer. *Nat. Rev. Cancer*, 392–401. doi:10.1038/nrc1877 (2006).
- [38] Pinchuk, I. V. *et al.* PD-1 Ligand Expression by Human Colonic Myofibroblasts/Fibroblasts Regulates CD4+ T-Cell Activity. *Gastroenterology* **135**, 1228–1237.e2. doi:10.1053/j.gastro.2008.07.016 (Oct. 2008).
- [39] Costa, A. *et al.* Fibroblast Heterogeneity and Immunosuppressive Environment in Human Breast Cancer. *Cancer Cell*. doi:10.1016/j.ccell.2018.01.011 (Mar. 2018).
- [40] Mantovani, A., Allavena, P., Sica, A. & Balkwill, F. Cancer-related inflammation. *Nature* **454**, 436–444. doi:10.1038/nature07205 (July 2008).
- [41] Ugel, S., Sanctis, F. D., Mandruzzato, S. & Bronte, V. Tumor-induced myeloid deviation: when myeloid-derived suppressor cells meet tumor-associated macrophages. *J. Clin. Invest.* **125**, 3365–3376. doi:10.1172/jci80006 (Sept. 2015).
- [42] Mantovani, A., Marchesi, F., Malesci, A., Laghi, L. & Allavena, P. Tumour-associated macrophages as treatment targets in oncology. *Nat. Rev. Clin. Oncol.* **14**, 399–416. doi:10.1038/nrclinonc.2016.217 (Jan. 2017).

- [43] Chitu, V. & Stanley, E. R. Colony-stimulating factor-1 in immunity and inflammation. *Curr. Opin. Immunol.* **18**, 39–48. doi:10.1016/j.coi.2005.11.006 (Feb. 2006).
- [44] Corriden, R. & Insel, P. A. Basal Release of ATP: An Autocrine-Paracrine Mechanism for Cell Regulation. *Sci. Signal.* **3**, re1–re1. doi:10.1126/scisignal.3104re1 (Jan. 2010).
- [45] Bours, M., Swennen, E., Virgilio, F. D., Cronstein, B. & Dagnelie, P. Adenosine 5'-triphosphate and adenosine as endogenous signaling molecules in immunity and inflammation. *Pharmacol. Ther.* **112**, 358–404. doi:10.1016/j.pharmthera.2005.04.013 (Nov. 2006).
- [46] Yegutkin, G. G. Nucleotide- and nucleoside-converting ectoenzymes: Important modulators of purinergic signalling cascade. *Biochim. Biophys. Acta, Mol. Cell Res.* **1783**, 673–694. doi:10.1016/j.bbamcr.2008.01.024 (May 2008).
- [47] Ferretti, E., Horenstein, A., Canzonetta, C., Costa, F. & Morandi, F. Canonical and non-canonical adenosinergic pathways. *Immunol. Lett.* **205**, 25–30. doi:10.1016/j.imlet.2018.03.007 (Jan. 2019).
- [48] Allard, B., Longhi, M. S., Robson, S. C. & Stagg, J. The ectonucleotidases CD39 and CD73: Novel checkpoint inhibitor targets. *Immunol. Rev.* **276**, 121–144. doi:10.1111/imr.12528 (Mar. 2017).
- [49] Deaglio, S. *et al.* Adenosine generation catalyzed by CD39 and CD73 expressed on regulatory T cells mediates immune suppression. *J. Exp. Med.* **204**, 1257–1265. doi:10.1084/jem.20062512 (May 2007).
- [50] Kukulski, F., Lévesque, S. A. & Sévigny, J. Impact of Ectoenzymes on P2 and P1 Receptor Signaling. *Adv. Pharmacol.* 263–299. doi:10.1016/b978-0-12-385526-8.00009-6 (2011).
- [51] Abbracchio, M. P., Burnstock, G., Verkhratsky, A. & Zimmermann, H. Purinergic signalling in the nervous system: an overview. *Trends Neurosci.* **32**, 19–29. doi:10.1016/j.tins.2008.10.001 (Jan. 2009).
- [52] Barrett, M. O. *et al.* A Selective High-Affinity Antagonist of the P2Y₁₄ Receptor Inhibits UDP-Glucose-Stimulated Chemotaxis of Human Neutrophils. *Mol. Pharmacol.* **84**, 41–49. doi:10.1124/mol.113.085654 (Apr. 2013).
- [53] Marteau, F., Communi, D., Boeynaems, J.-M. & Gonzalez, N. S. Involvement of multiple P2Y receptors and signaling pathways in the action of adenine nucleotides diphosphates on human monocyte-derived dendritic cells. *J. Leukocyte Biol.* **76**, 796–803. doi:10.1189/jlb.0104032 (July 2004).
- [54] Beldi, G. *et al.* Natural killer T cell dysfunction in CD39-null mice protects against concanavalin A-induced hepatitis. *Hepatology* **48**, 841–852. doi:10.1002/hep.22401 (Sept. 2008).
- [55] Wirkner, K., Sperlagh, B. & Illes, P. P2X₃ Receptor Involvement in Pain States. *Mol. Neurobiol.* **36**, 165–183. doi:10.1007/s12035-007-0033-y (July 2007).

- [56] Liu, X., Ma, L., Zhang, S., Ren, Y. & Dirksen, R. CD73 Controls Extracellular Adenosine Generation in the Trigeminal Nociceptive Nerves. *J. Dent. Res.* **96**, 671–677. doi:10.1177/0022034517692953 (Feb. 2017).
- [57] Koonin, E. V. Conserved sequence pattern in a wide variety of phosphoesterases. *Protein Sci.* **3**, 356–358. doi:10.1002/pro.5560030218 (Dec. 1994).
- [58] Martinez–Martinez, A. *et al.* The ecto-5′-nucleotidase subunits in dimers are not linked by disulfide bridges but by non-covalent bonds. *Biochim. Biophys. Acta, Protein Struct. Mol. Enzymol.* **1478**, 300–308. doi:10.1016/s0167-4838(00)00035-2 (May 2000).
- [59] Airas, L., Niemelä, J., Salmi, M., Puurunen, T., Smith, D. J. & Jalkanen, S. Differential Regulation and Function of CD73, a Glycosyl-Phosphatidylinositol-linked 70-kD Adhesion Molecule, on Lymphocytes and Endothelial Cells. *J. Cell Biol.* **136**, 421–431. doi:10.1083/jcb.136.2.421 (Jan. 1997).
- [60] Maksimow, M. *et al.* Early Prediction of Persistent Organ Failure by Soluble CD73 in Patients With Acute Pancreatitis. *Crit. Care Med.* **42**, 2556–2564. doi:10.1097/ccm.0000000000000550 (Dec. 2014).
- [61] Liu, H. *et al.* Elevated ecto-5′-nucleotidase: a missing pathogenic factor and new therapeutic target for sickle cell disease. *Blood Adv.* **2**, 1957–1968. doi:10.1182/bloodadvances.2018015784 (Aug. 2018).
- [62] Huang, Q. *et al.* Abstract 1538: Levels and enzyme activity of CD73 in primary samples from cancer patients. *Cancer Res.* **75**, 1538–1538. doi:10.1158/1538-7445.am2015-1538 (Aug. 2015).
- [63] Morello, S. *et al.* Soluble CD73 as biomarker in patients with metastatic melanoma patients treated with nivolumab. *J. Transl. Med.* **15**. doi:10.1186/s12967-017-1348-8 (Dec. 2017).
- [64] Yegutkin, G. G. *et al.* Ecto-5′-nucleotidase/CD73 enhances endothelial barrier function and sprouting in blood but not lymphatic vasculature. *Eur. J. Immunol.* **45**, 562–573. doi:10.1002/eji.201444856 (Dec. 2014).
- [65] Walldén, K. *et al.* Crystal Structure of Human Cytosolic 5′-Nucleotidase II. *J. Biol. Chem.* **282**, 17828–17836. doi:10.1074/jbc.m700917200 (Apr. 2007).
- [66] Sträter, N. & Knöfel, T. X-ray structure of the Escherichia coli periplasmic 5′-nucleotidase containing a dimetal catalytic site. *Nat. Struct. Biol.* **6**, 448–453. doi:10.1038/8253 (May 1999).
- [67] Patskovsky, Y. *et al.* Crystal structure of 5′-nucleotidase from *Candida albicans* SC5314 Feb. 2008. doi:10.2210/pdb3c9f/pdb.
- [68] Knapp, K., Zebisch, M., Pippel, J., El-Tayeb, A., Müller, C. E. & Sträter, N. Crystal Structure of the Human Ecto-5′-Nucleotidase (CD73): Insights into the Regulation of Purinergic Signaling. *Structure* **20**, 2161–2173. doi:10.1016/j.str.2012.10.001 (Dec. 2012).
- [69] Heuts, D. P. H. M. *et al.* Crystal Structure of a Soluble Form of Human CD73 with Ecto-5′-Nucleotidase Activity. *ChemBioChem* **13**, 2384–2391. doi:10.1002/cbic.201200426 (Sept. 2012).

- [70] Kamariah, N., Eisenhaber, F., Adhikari, S., Eisenhaber, B. & Grüber, G. Purification and crystallization of yeast glycosylphosphatidylinositol transamidase subunit PIG-S (PIG-S71–467). *Acta Crystallogr. Sect. F Struct. Biol. Cryst. Commun.* **67**, 896–899. doi:10.1107/s1744309111024080 (July 2011).
- [71] Paulick, M. G. & Bertozzi, C. R. The Glycosylphosphatidylinositol Anchor: A Complex Membrane-Anchoring Structure for Proteins. *Biochemistry* **47**, 6991–7000. doi:10.1021/bi8006324 (July 2008).
- [72] Knöfel, T. & Sträter, N. Mechanism of hydrolysis of phosphate esters by the dimetal center of 5′-nucleotidase based on crystal structures. *J. Mol. Biol.* **309**, 239–254. doi:10.1006/jmbi.2001.4656 (May 2001).
- [73] McMillen, L., Beacham, I. R. & Burns, D. M. Cobalt activation of Escherichia coli 5′-nucleotidase is due to zinc ion displacement at only one of two metal-ion-binding sites. *Biochem. J.* **372**, 625–630. doi:10.1042/bj20021800 (June 2003).
- [74] Sträter, N. Ecto-5′-nucleotidase: Structure function relationships. *Purinergic Signal.* **2**, 343–350. doi:10.1007/s11302-006-9000-8 (May 2006).
- [75] Sadej, R. & Skladanowski, A. C. Dual, enzymatic and non-enzymatic, function of ecto-5′-nucleotidase (eN, CD73) in migration and invasion of A375 melanoma cells. *Acta Biochim. Pol.* **59**. doi:10.18388/abp.2012_2105 (Nov. 2012).
- [76] Garavaglia, S. *et al.* The high-resolution crystal structure of periplasmic Haemophilus influenzae NAD nucleotidase reveals a novel enzymatic function of human CD73 related to NAD metabolism. *Biochem. J.* **441**, 131–141. doi:10.1042/bj20111263 (Jan. 2012).
- [77] Grondal, E. J. M. & Zimmermann, H. Purification, characterization and cellular localization of 5′-nucleotidase from Torpedoelectric organ. *Biochem. J.* **245**, 805–810. doi:10.1042/bj2450805 (Aug. 1987).
- [78] Bhattarai, S. *et al.* α , β -Methylene-ADP (AOPCP) Derivatives and Analogues: Development of Potent and Selective ecto-5′-Nucleotidase (CD73) Inhibitors. *J. Med. Chem.* **58**, 6248–6263. doi:10.1021/acs.jmedchem.5b00802 (July 2015).
- [79] Braganhol, E., Tamajusuku, A. S., Bernardi, A., Wink, M. R. & Battastini, A. M. Ecto-5′-nucleotidase/CD73 inhibition by quercetin in the human U138MG glioma cell line. *Biochim. Biophys. Acta Gen. Subj.* **1770**, 1352–1359. doi:10.1016/j.bbagen.2007.06.003 (Sept. 2007).
- [80] Baqi, Y. *et al.* Development of Potent and Selective Inhibitors of ecto-5′-Nucleotidase Based on an Anthraquinone Scaffold. *J. Med. Chem.* **53**, 2076–2086. doi:10.1021/jm901851t (Mar. 2010).
- [81] Ripphausen, P., Freundlieb, M., Brunschweiler, A., Zimmermann, H., Müller, C. E. & Bajorath, J. Virtual Screening Identifies Novel Sulfonamide Inhibitors of ecto-5′-Nucleotidase. *J. Med. Chem.* **55**, 6576–6581. doi:10.1021/jm300658n (July 2012).

- [82] Tan, J. *et al.* *Preclinical Pharmacokinetic and Pharmacodynamic Characterization of AB680, a Small-Molecule CD73 Inhibitor for Cancer Immunotherapy.* in *International Cancer Immunotherapy Conference: Translating Science into Survival* (Oct. 3, 2018). <https://www.arcusbio.com/wp-content/uploads/2018/10/2018.09-CRI-AB680-Preclinical-Profile-poster.pdf>.
- [83] Stagg, J. *et al.* Anti-CD73 antibody therapy inhibits breast tumor growth and metastasis. *Proc. Natl. Acad. Sci.* **107**, 1547–1552. doi:10.1073/pnas.0908801107 (Jan. 2010).
- [84] Geoghegan, J. C. *et al.* Inhibition of CD73 AMP hydrolysis by a therapeutic antibody with a dual, non-competitive mechanism of action. *mAbs* **8**, 454–467. doi:10.1080/19420862.2016.1143182 (Feb. 2016).
- [85] Zhou, P. *et al.* Overexpression of Ecto-5'-Nucleotidase (CD73) promotes T-47D human breast cancer cells invasion and adhesion to extracellular matrix. *Cancer Biol. Ther.* **6**, 426–431. doi:10.4161/cbt.6.3.3762 (Mar. 2007).
- [86] Airas, L. CD73 is involved in lymphocyte binding to the endothelium: characterization of lymphocyte-vascular adhesion protein 2 identifies it as CD73. *J. Exp. Med.* **182**, 1603–1608. doi:10.1084/jem.182.5.1603 (Nov. 1995).
- [87] Dianzani, U. *et al.* Co-stimulatory signal delivered by CD73 molecule to human CD45RAhiCD45ROlo (naive) CD8+ T lymphocytes. *J. Immunol.* **151**, 3961–3970. ISSN: 0022-1767. eprint: <http://www.jimmunol.org/content/151/8/3961.full.pdf>. <http://www.jimmunol.org/content/151/8/3961> (Oct. 1993).
- [88] Gutensohn, W., Resta, R., Misumi, Y., Ikehara, Y. & Thompson, L. F. Ecto-5'-nucleotidase Activity Is Not Required for T Cell Activation through CD73. *Cell. Immunol.* **161**, 213–217. doi:10.1006/cimm.1995.1029 (Apr. 1995).
- [89] MIT & Harvard. [Online]. *GTEx Portal* <https://gtexportal.org/home/>. [Cited on Apr. 10, 2019].
- [90] Carithers, L. J. & Moore, H. M. The Genotype-Tissue Expression (GTEx) Project. *Biopreserv. Biobanking* **13**, 307–308. doi:10.1089/bio.2015.29031.hmm (Oct. 2015).
- [91] Lizio, M. *et al.* Update of the FANTOM web resource: high resolution transcriptome of diverse cell types in mammals. *Nucleic Acids Res.* **45**, D737–D743. doi:10.1093/nar/gkw995 (Oct. 2016).
- [92] [Online]. *Human Protein Atlas* version 18.1. <https://www.proteinatlas.org>. [Cited on Apr. 9, 2019].
- [93] Uhlen, M. *et al.* Tissue-based map of the human proteome. *Science* **347**, 1260419–1260419. doi:10.1126/science.1260419 (Jan. 2015).
- [94] Otsuki, T. Signal Sequence and Keyword Trap in silico for Selection of Full-Length Human cDNAs Encoding Secretion or Membrane Proteins from Oligo-Capped cDNA Libraries. *DNA Res.* **12**, 117–126. doi:10.1093/dnares/12.2.117 (Jan. 2005).

- [95] Snider, N. T., Altshuler, P. J., Wan, S., Welling, T. H., Cavalcoli, J. & Omary, M. B. Alternative splicing of human NT5E in cirrhosis and hepatocellular carcinoma produces a negative regulator of ecto-5'-nucleotidase (CD73). *Mol. Biol. Cell* **25**, 4024–4033. doi:10.1091/mbc.e14-06-1167 (Dec. 2014).
- [96] Colgan, S. P., Eltzschig, H. K., Eckle, T. & Thompson, L. F. Physiological roles for ecto-5'-nucleotidase (CD73). *Purinergic Signal.* **2**, 351–360. doi:10.1007/s11302-005-5302-5 (June 2006).
- [97] Strohmeier, G. R. *et al.* Surface expression, polarization, and functional significance of CD73 in human intestinal epithelia. *J. Clin. Invest.* **99**, 2588–2601. doi:10.1172/jci119447 (June 1997).
- [98] Weissmuller, T., Eltzschig, H. K. & Colgan, S. P. Dynamic purine signaling and metabolism during neutrophil–endothelial interactions. *Purinergic Signal.* **1**, 229–239. doi:10.1007/s11302-005-6323-9 (July 2005).
- [99] Thompson, L. F. *et al.* Crucial Role for Ecto-5'-Nucleotidase (CD73) in Vascular Leakage during Hypoxia. *J. Exp. Med.* **200**, 1395–1405. doi:10.1084/jem.20040915 (Dec. 2004).
- [100] Synnestvedt, K. *et al.* Ecto-5'-nucleotidase (CD73) regulation by hypoxia-inducible factor-1 mediates permeability changes in intestinal epithelia. *J. Clin. Invest.* **110**, 993–1002. doi:10.1172/jci0215337 (Oct. 2002).
- [101] Spychala, J. Role of Estrogen Receptor in the Regulation of Ecto-5'-Nucleotidase and Adenosine in Breast Cancer. *Clin. Cancer Res.* **10**, 708–717. doi:10.1158/1078-0432.ccr-0811-03 (Jan. 2004).
- [102] Hansen, K. R., Resta, R., Webb, C. F. & Thompson, L. F. Isolation and characterization of the promoter of the human 5'-nucleotidase (CD73)-encoding gene. *Gene* **167**, 307–312. doi:10.1016/0378-1119(95)00574-9 (Dec. 1995).
- [103] Thompson, L. F., Ruedi, J. M., O'Connor, R. D. & Bastian, J. F. Ecto-5'-nucleotidase expression during human B cell development. An explanation for the heterogeneity in B lymphocyte ecto-5'-nucleotidase activity in patients with hypogammaglobulinemia. *J. Immunol.* **137**, 2496–2500. ISSN: 0022-1767 (8 Oct. 1986).
- [104] Resta, R., Yamashita, Y. & Thompson, L. F. Ecto-enzyme and signaling functions of lymphocyte CD73. *Immunol. Rev.* **161**, 95–109. doi:10.1111/j.1600-065x.1998.tb01574.x (Feb. 1998).
- [105] Antonioli, L., Pacher, P., Vizi, E. S. & Haskó, G. CD39 and CD73 in immunity and inflammation. *Trends Mol. Med.* **19**, 355–367. doi:10.1016/j.molmed.2013.03.005 (June 2013).
- [106] Zanin, R. F. *et al.* Differential Macrophage Activation Alters the Expression Profile of NTPDase and Ecto-5'-Nucleotidase. *PLoS ONE* **7**, e31205. doi:10.1371/journal.pone.0031205 (Feb. 2012).
- [107] Mandapathil, M. *et al.* Generation and Accumulation of Immunosuppressive Adenosine by Human CD4⁺CD25^{high}FOXP3⁺Regulatory T Cells. *J. Biol. Chem.* **285**, 7176–7186. doi:10.1074/jbc.m109.047423 (Oct. 2009).

- [108] Chalmin, F. *et al.* Stat3 and Gfi-1 Transcription Factors Control Th17 Cell Immunosuppressive Activity via the Regulation of Ectonucleotidase Expression. *Immunity* **36**, 362–373. doi:10.1016/j.immuni.2011.12.019 (Mar. 2012).
- [109] Regateiro, F. S., Cobbold, S. P. & Waldmann, H. CD73 and adenosine generation in the creation of regulatory microenvironments. *Clin. Exp. Immunol.* **171**, 1–7. doi:10.1111/j.1365-2249.2012.04623.x (Dec. 2012).
- [110] Bono, M. R., Fernández, D., Flores-Santibáñez, F., Roseblatt, M. & Sauma, D. CD73 and CD39 ectonucleotidases in T cell differentiation: Beyond immunosuppression. *FEBS Letters* **589**, 3454–3460. doi:10.1016/j.febslet.2015.07.027 (July 2015).
- [111] Anderson, S. M., Tomayko, M. M., Ahuja, A., Haberman, A. M. & Shlomchik, M. J. New markers for murine memory B cells that define mutated and unmutated subsets. *J. Exp. Med.* **204**, 2103–2114. doi:10.1084/jem.20062571 (Aug. 2007).
- [112] Kaku, H., Cheng, K. F., Al-Abed, Y. & Rothstein, T. L. A Novel Mechanism of B Cell-Mediated Immune Suppression through CD73 Expression and Adenosine Production. *J. Immunol.* **193**, 5904–5913. doi:10.4049/jimmunol.1400336 (Nov. 2014).
- [113] Mauri, C. & Menon, M. The expanding family of regulatory B cells. *Int. Immunol.* **27**, 479–486. doi:10.1093/intimm/dxv038 (June 2015).
- [114] Chatterjee, D., Tufa, D. M., Baehre, H., Hass, R., Schmidt, R. E. & Jacobs, R. Natural killer cells acquire CD73 expression upon exposure to mesenchymal stem cells. *Blood* **123**, 594–595. doi:10.1182/blood-2013-09-524827.
- [115] Airas, L. & Jalkanen, S. CD73 mediates adhesion of B cells to follicular dendritic cells. *Blood* **88**, 1755–1764. ISSN: 0006-4971 (5 Sept. 1996).
- [116] Airas, L. CD73 and Adhesion of B-Cells to Follicular Dendritic Cells. *Leuk. Lymphoma* **29**, 37–47. doi:10.3109/10428199809058380 (Jan. 1998).
- [117] Hilaire, C. S. *et al.* NT5E Mutations and Arterial Calcifications. *N. Engl. J. Med.* **364**, 432–442. doi:10.1056/nejmoa0912923 (Feb. 2011).
- [118] Fausther, M., Lavoie, E. G., Goree, J. R., Baldini, G. & Dranoff, J. A. NT5E Mutations That Cause Human Disease Are Associated with Intracellular Mistrafficking of NT5E Protein. *PLoS ONE* **9**, e98568. doi:10.1371/journal.pone.0098568 (June 2014).
- [119] Antonioli, L., Yegutkin, G. G., Pacher, P., Blandizzi, C. & Haskó, G. Anti-CD73 in Cancer Immunotherapy: Awakening New Opportunities. *Trends Cancer* **2**, 95–109. doi:10.1016/j.trecan.2016.01.003 (Feb. 2016).
- [120] Wang, H. *et al.* NT5E (CD73) is epigenetically regulated in malignant melanoma and associated with metastatic site specificity. *Br. J. Cancer* **106**, 1446–1452. doi:10.1038/bjc.2012.95 (Mar. 2012).

- [121] Allard, B., Turcotte, M. & Stagg, J. Targeting CD73 and downstream adenosine receptor signaling in triple-negative breast cancer. *Expert Opin. Ther. Targets* **18**, 863–881. doi:10.1517/14728222.2014.915315 (May 2014).
- [122] Loi, S. *et al.* CD73 promotes anthracycline resistance and poor prognosis in triple negative breast cancer. *Proc. Natl. Acad. Sci.* **110**, 11091–11096. doi:10.1073/pnas.1222251110 (June 2013).
- [123] Nigro, C. L. *et al.* NT5E CpG island methylation is a favourable breast cancer biomarker. *Br. J. Cancer* **107**, 75–83. doi:10.1038/bjc.2012.212 (May 2012).
- [124] Yang, Q., Du, J. & Zu, L. Overexpression of CD73 in Prostate Cancer is Associated with Lymph Node Metastasis. *Pathol. Oncol. Res.* **19**, 811–814. doi:10.1007/s12253-013-9648-7 (May 2013).
- [125] Sitkovsky, M. V., Hatfield, S., Abbott, R., Belikoff, B., Lukashev, D. & Ohta, A. Hostile, Hypoxia-A2-Adenosinergic Tumor Biology as the Next Barrier to Overcome for Tumor Immunologists. *Cancer Immunol. Res.* **2**, 598–605. doi:10.1158/2326-6066.cir-14-0075 (July 2014).
- [126] Reinhardt, J. *et al.* MAPK Signaling and Inflammation Link Melanoma Phenotype Switching to Induction of CD73 during Immunotherapy. *Cancer Res.* **77**, 4697–4709. doi:10.1158/0008-5472.can-17-0395 (June 2017).
- [127] Samanta, D. *et al.* Chemotherapy induces enrichment of CD47⁺/CD73⁺/PDL1⁺ immune evasive triple-negative breast cancer cells. *Proc. Natl. Acad. Sci.* **115**, E1239–E1248. doi:10.1073/pnas.1718197115 (Jan. 2018).
- [128] Bowser, J. L. & Broaddus, R. R. CD73s protection of epithelial integrity: Thinking beyond the barrier. *Tissue Barriers* **4**, e1224963. doi:10.1080/21688370.2016.1224963 (Aug. 2016).
- [129] Gordon, L. A., Mulligan, K. T., Maxwell-Jones, H., Adams, M., Walker, R. A. & Jones, J. L. Breast cell invasive potential relates to the myoepithelial phenotype. *Int. J. Cancer* **106**, 8–16. doi:10.1002/ijc.11172 (June 2003).
- [130] Leth-Larsen, R. *et al.* Metastasis-related Plasma Membrane Proteins of Human Breast Cancer Cells Identified by Comparative Quantitative Mass Spectrometry. *Mol. Cell. Proteomics* **8**, 1436–1449. doi:10.1074/mcp.m800061-mcp200 (Mar. 2009).
- [131] Supernat, A. *et al.* CD73 Expression as a Potential Marker of Good Prognosis in Breast Carcinoma. *Appl. Immunohistochem. Mol. Morphol.* **20**, 103–107. doi:10.1097/pai.0b013e3182311d82 (Mar. 2012).
- [132] Wang, L. *et al.* CD73 has distinct roles in nonhematopoietic and hematopoietic cells to promote tumor growth in mice. *J. Clin. Invest.* **121**, 2371–2382. doi:10.1172/jci45559 (June 2011).
- [133] Hay, C. M. *et al.* Targeting CD73 in the tumor microenvironment with MEDI9447. *OncoImmunology* **5**, e1208875. doi:10.1080/2162402x.2016.1208875 (July 2016).

- [134] Siu, L. L. *et al.* Abstract CT180: Preliminary phase 1 profile of BMS-986179, an anti-CD73 antibody, in combination with nivolumab in patients with advanced solid tumors. *Cancer Res.* **78**, CT180–CT180. doi:10.1158/1538-7445.am2018-ct180 (July 2018).
- [135] Šácha, P. *et al.* iBodies: Modular Synthetic Antibody Mimetics Based on Hydrophilic Polymers Decorated with Functional Moieties. *Angew. Chem. Int. Ed.* **55**, 2356–2360. doi:10.1002/anie.201508642 (Jan. 2016).
- [136] Šprincl, L., Vacik, J., Kopecek, J. & Lim, D. Biological tolerance of poly(N-substituted methacrylamides). *J. Biomed. Mater. Res.* **5**, 197–205. doi:10.1002/jbm.820050307 (May 1971).
- [137] Ulbrich, K. & Šubr, V. Structural and chemical aspects of HPMA copolymers as drug carriers. *Adv. Drug Delivery Rev.* **62**, 150–166. doi:10.1016/j.addr.2009.10.007 (Feb. 2010).
- [138] Durocher, Y., Perret, S. & Kamen, A. High-level and high-throughput recombinant protein production by transient transfection of suspension-growing human 293-EBNA1 cells. *Nucleic Acids Res.* **30**, 9e–9. doi:10.1093/nar/30.2.e9 (Jan. 2002).
- [139] Bradford, M. M. A rapid and sensitive method for the quantitation of microgram quantities of protein utilizing the principle of protein-dye binding. *Anal. Biochem.* **72**, 248–254. doi:10.1016/0003-2697(76)90527-3 (May 1976).
- [140] Navrátil, V. *et al.* DNA-linked Inhibitor Antibody Assay (DIANA) for sensitive and selective enzyme detection and inhibitor screening. *Nucleic Acids Res.* **45**, e10–e10. doi:10.1093/nar/gkw853 (Sept. 2016).
- [141] Šimonová, L. *Preparation of glutamate carboxypeptidase III using mammalian expression system* Bachelor thesis (2017).

List of Figures

1	Overview of leukocyte types	13
2	Role of immune checkpoint inhibitors	16
3	Purinoreceptors	18
4	Structure of CD73	19
5	Structure of active site of CD73 with AOPCP	20
6	Inhibitors of CD73	21
7	Cells expressing CD73	23
8	Schematic structure of HPMA	25
9	Plasmid maps used for cloning	30
10	Example of gating in FACSDiva software	40
11	Agarose electrophoresis	41
12	Small-scale transfection 1	42
13	Small-scale transfection 2	42
14	Purification I	43
15	Purification II	43
16	Michaelis constant of rhCD73	44
17	Inhibition of rhCD73 by PSB12379	45
18	Structure of inhibitors PSI397 and PSI405	45
19	Inhibition of rhCD73 by PSI397 and P4 probe	46
20	Structure of inhibitor PSI389	47
21	Polymer binding curve on rhCD73 in ELISA	48
22	Specific polymer binding on CD73+ cells	49
23	Binding curve of anti-CD73 iBody on expressing and non-expressing cells	49

List of Tables

1	Conditions of polymerase chain reaction.	31
2	Reaction mixture of ligation reaction.	31
3	Overview of washing and elution fractions during first and second round of purification.	34
4	Concentration and purity of prepared plasmids, measured on NanoDrop.	41
5	Amount of CD73 in different fractions.	44
6	Overview of DIANA optimisation	46
7	Sequences of primers used for PCR and sequencing.	55
8	Condition of cleavage by restriction endonucleases.	55